Robust Non-Destructive Prediction of Jackfruit (Artocarpus heterophyllus cv. Tekam Yellow) Colour at Different Maturity Stages Using Visible–Near Infrared Spectroscopy: Influence of Rind and Flesh

Kok Jeng Lim
limkokjeng@gmail.com

Universiti Putra Malaysia

Phebe Ding
Universiti Putra Malaysia

Nazmi Mat Nawi
Universiti Putra Malaysia

Mashitah Jusoh
Universiti Putra Malaysia

Research Article

Keywords: jackfruit, robust predicting, Pantoea stewartii, visible near infrared spectroscopy (Vis-NIRS), intact, fruit bronzing, colour metrics

Posted Date: April 1st, 2026

DOI: https://doi.org/10.21203/rs.3.rs-9106139/v1

Additional Declarations: No competing interests reported.

Robust Non-Destructive Prediction of Jackfruit (*Artocarpus heterophyllus* cv. Tekam Yellow) Colour at Different Maturity Stages Using Visible–Near Infrared Spectroscopy: Influence of Rind and Flesh

Kok Jeng Lim[1], Phebe Ding[1], Nazmi Mat Nawi[2,3] and Mashitah Jusoh[1]
[1]Department of Crop Science, Faculty of Agriculture, Universiti Putra Malaysia, 43400 UPM Serdang, Selangor Malaysia.
[2]Department of Biological and Agricultural Engineering, Faculty of Engineering, Universiti Putra Malaysia, 43400 UPM Serdang, Selangor, Malaysia.
[3]Institute of Plantation Studies, Universiti Putra Malaysia, 43400 UPM Serdang, Selangor, Malaysia.
Email addresses: gs60341@student.upm.edu.my, phebe@upm.edu.my, nazmimat@upm.edu.my, mashitahj@upm.edu.my,

Corresponding Author:
Name: Kok Jeng Lim
Email: limkokjeng@gmail.com

Abstract

The Malaysian jackfruit (*Artocarpus heterophyllus*) industry is increasingly challenged by a physiological disorder known as *jackfruit bronzing*, attributed to *Pantoea stewartii* subsp. *stewartii*. This disorder manifests as a yellowish-orange to reddish discolouration of the pulp while leaving the rind visually unaffected, leading to substantial postharvest quality and economic losses. The *Tekam Yellow* cultivar, in particular, has demonstrated high susceptibility to this condition. This study aimed to evaluate the potential of visible near-infrared spectroscopy (Vis–NIRS) as a non-destructive analytical tool for the early detection of internal bronzing through the estimation of rind and flesh colour parameters (L*, a*, b*, C*, ΔE, and h°). Spectral data were collected from the rind surface of intact jackfruit samples at 10, 12, and 14 weeks after anthesis (WAA) across the 500–950 nm wavelength range. Partial Least Squares Regression (PLSR) models were developed to establish the relationship between spectral reflectance and reference colour metrics. Various spectral pre-processing techniques—including Savitzky–Golay smoothing, Standard Normal Variate (SNV), and Multiplicative Scatter Correction (MSC)—were applied to enhance signal quality and minimise scattering effects. The optimised models demonstrated high predictive accuracy, with coefficients of determination for calibration (Rc^2) and prediction (Rp^2) reaching up to 0.98. Correspondingly, root mean square errors of calibration (RMSEC) and prediction (RMSEP) were as low as 0.29. Overall, calibration performance remained consistently strong across traits and maturities ($Rc^2 \geq 0.62$), indicating that the model structures effectively captured the spectral–colour relationships within the calibration dataset. In contrast, the predictive performance of independent validation models varied substantially between normal and bronzing conditions. Under normal conditions, several models achieved excellent predictive accuracy—for instance, rind colour L* at 10 WAA ($Rp^2 = 0.95$, RPD = 16.19) and flesh colour L* at 10 WAA ($Rp^2 = 0.98$, RPD = 10.88). Conversely, models developed under bronzing conditions frequently exhibited lower predictive coefficients (Rp^2) and residual predictive deviation (RPD) values (< 1.0), suggesting greater spectral heterogeneity and reduced stability in diseased tissues.These findings imply that while overfitting was not evident during calibration, the spectral–chemical mapping was less robust under pathological or variable maturity conditions, thereby reducing external validity. Complementary destructive reference measurements were conducted and analysed using analysis of variance (ANOVA) followed by Fisher's Protected Least Significant Difference (FPLSD) test at $p \leq 0.05$ to confirm the significance of observed differences. Collectively, the results demonstrate that Vis–NIRS applied through the rind offers a promising non-invasive approach for the rapid and accurate detection of internal bronzing in *Tekam Yellow* jackfruit, facilitating improved quality monitoring and early disease detection at both harvest and postharvest stages. This work highlights the potential of Vis–NIRS as a practical, high-throughput

phenotyping and quality assurance tool to support sustainable value-chain management in the Malaysian jackfruit industry.

Keywords: jackfruit, robust predicting, *Pantoea stewartii*, visible near infrared spectroscopy (Vis-NIRS), intact, fruit bronzing, colour metrics

1. Introduction

Visible near-infrared (Vis-NIR) spectroscopy has become an increasingly prominent analytical technique for evaluating internal quality attributes in agricultural produce. Its rapid, non-destructive, and reagent-free nature has made it especially valuable for postharvest quality control, grading, and storage management [25]. Over the past decade, Vis-NIR spectroscopy has been successfully applied to a range of fruit species, including apples [20, 25, 34 & 42], kiwifruit [4, 40 & 50], citrus [29 & 33], mango [6 & 60], durian [49], pear [14 & 47], and grape [19]. These studies collectively demonstrate the technology's capacity to predict internal attributes such as colour, firmness, soluble solids content (SSC), and titratable acidity with high precision, even under variable environmental or physiological conditions [7, 24, 27 & 32].

Despite its broad application across fruit species, *Artocarpus heterophyllus* Lam. cv. Tekam Yellow (jackfruit) remains underrepresented in Vis-NIR research, particularly concerning internal physiological disorders such as bronzing. Bronzing disorder is a serious postharvest issue caused by *Pantoea stewartii* subsp. *stewartii*, often associated with *ChrysSA* sp. flea beetles [28]. The disease affects internal tissues—particularly the pulp and rags—without exhibiting visible external symptoms. Internally, affected fruits display yellowish-orange to reddish discoloration with rust-like specks [3, 30 & 69], leading to reduced consumer acceptance and marketability despite minimal changes in taste or nutritional quality [21 & 28]. Conventional destructive assessment methods, such as slicing or juicing, are not only labour-intensive but also ineffective in detecting hidden internal disorders. Consequently, the development of non-invasive and rapid diagnostic tools is crucial for enhancing quality assurance in the jackfruit supply chain.

The accuracy of Vis-NIR models, however, is often influenced by biological variability, including cultivar differences, environmental stress, and disease incidence, which can alter spectral reflectance and scattering properties [23 & 52]. These sources of variation challenge the stability of predictive models, especially for fruits with heterogeneous structures such as jackfruit. To address these complexities, multivariate regression methods—particularly partial least squares regression (PLSR)—are widely employed. PLSR effectively manages the collinearity inherent in spectral datasets by projecting predictor variables into a reduced latent space that maximizes covariance with the response variables [44]. This capability enables robust model calibration and enhances interpretability compared to principal components regression [10]. Complementary statistical tools such as analysis of variance (ANOVA) and other multivariate techniques further assist in identifying factors affecting model performance and calibration reliability [59 & 68].

While full-range Vis-NIR spectra provide abundant chemical and physical information, many wavelengths may contribute little or even introduce noise into predictive models [67]. Therefore, feature selection and variable reduction are critical to isolate informative bands and enhance both computational efficiency and predictive accuracy [31]. Equally important is the use of spectral preprocessing techniques to mitigate unwanted variations caused by light scattering, baseline shifts, and instrument drift [55]. Such pretreatments—commonly including smoothing, standard normal variate (SNV), and multiplicative scatter correction (MSC)—are essential for improving the signal-to-noise ratio and enhancing calibration robustness.

In this study, twelve different preprocessing combinations were systematically evaluated, encompassing three smoothing filters (Savitzky–Golay, Gaussian, and Median) combined with SNV and MSC in sequential or pairwise configurations. This methodological approach was designed to identify the optimal spectral conditioning strategy for predicting internal attributes across three jackfruit maturity stages (10, 12, and 14 weeks after anthesis) [2]. Although no prior study has tested twelve distinct pipelines, previous investigations have shown that the effectiveness of any single or combined preprocessing method depends on both the fruit matrix and analytical objective [43, 58 & 62]. Thus, a comprehensive evaluation of multiple combinations is justified to ensure generalizability and reduce overfitting in Vis-NIR-based predictive models.

The experimental design also emphasizes the importance of developing light-stable spectral acquisition protocols and rigorous chemometric frameworks for non-destructive fruit analysis. Parameters measured include rind and flesh colour metrics (L*, a*, b*, C*, ΔE, and h°), while model development focuses on classifying fruit condition (healthy versus bronzed) using PLSR. By investigating how biological variability, instrumental parameters, and measurement conditions influence model robustness, the study seeks to refine the predictive capacity of Vis-NIR spectroscopy for tropical fruits.

Overall, this research aims to: (i) develop a stable Vis-NIR experimental protocol suitable for large, heterogeneous fruits such as jackfruit; (ii) construct robust PLSR-based models capable of discriminating between healthy and bronzing-affected fruits; and (iii) evaluate the impact of biological and instrumental variability on model performance. The outcomes are expected to contribute to a standardized methodological framework that enhances the reliability and scalability of Vis-NIR technology for non-destructive quality assessment in jackfruit, ultimately supporting its broader adoption in tropical fruit postharvest management systems.

2. Materials and methods

2.1 Plant material and harvesting stages

Jackfruit (*Artocarpus heterophyllus* Lam. cv. Tekam Yellow) samples were obtained from a commercial orchard operated by Agro BS Sdn. Bhd., Jasin, Melaka, Malaysia (2°23'31.5049" N, 102°25'7.4781" E). Across three harvesting seasons, 54 fruits (syncarps) were collected in three independent batches. Both bronzed and healthy fruits were sampled at three maturity stages: 10, 12, and 14 weeks after anthesis (WAA). For each maturity stage, six fruits per batch were harvested, placed in ventilated plastic sacks, and transported within two hours to Universiti Putra Malaysia for subsequent analyses.

2.2 Spectral acquisition

Spectral data of both rind and flesh were collected using a visible–near infrared (Vis–NIR) spectrometer (HR4000, Ocean Optics Inc., USA) operating in the 200–1100 nm range, with the analytical region limited to 500–950 nm. Measurements were performed in reflectance mode with a 1.5 cm scanning aperture. The halogen light source (HL-2000, Ocean Optics Inc., USA) was stabilised for 30 minutes before use.

A white reference (~100% reflectance) was recorded before each session, ensuring dust-free calibration. Spectra were captured in triplicate at the same position and averaged to obtain representative data. The setup comprised a high-resolution fibre optic probe (0.5 nm spectral resolution) housed in a light-proof black chamber to minimise ambient interference. All measurements were conducted in a dark room to enhance the signal-to-noise ratio. The same samples were later subjected to chemical analyses of rind and flesh quality parameters.

2.3 Refences methods rind and flesh colour

Spectral data were processed using *The Unscrambler X* version 10.3 (CAMO Software AS, Norway). The dataset was divided into calibration (75%) and validation (25%) subsets using an independent sample selection approach to ensure unbiased model assessment. The calibration subset was employed to construct regression models, whereas the validation subset was reserved for external performance testing. Model robustness was further examined through leave-one-out full cross-validation [7 & 64]. Prior to modelling, samples were sorted in ascending order based on colour metrics (L*, a*, b*, C*, ΔE, and h°) of both rind and flesh [7, 22 & 37], followed by random allocation by the software.

Considering that spectral features of intact jackfruit can be affected by surface roughness and thorn density, various spectral pre-processing techniques were evaluated to enhance signal quality and model accuracy. These included Savitzky–Golay smoothing, baseline correction, median filtering, Gaussian filtering, standard normal variate (SNV), and multiplicative signal correction (MSC) [1]. Partial Least Squares Regression (PLSR) was then applied to establish the quantitative relationship between the Vis–NIR spectra and the corresponding reference chemical parameters. This chemometric approach not only facilitates the quantification of targeted constituents but also enables the inference of their underlying chemical behaviours through spectral response patterns [63].

Analyses were restricted to the 500–950 nm spectral range, which corresponds to the Vis–NIR region most responsive to fruit biochemical attributes. Spectral datasets were pre-processed to remove noise and anomalous readings, with approximately 5% of extreme spectra excluded [2]. The refined dataset comprised 1,620 effective spectra from rind and flesh samples.

Model performance was evaluated based on several statistical indicators, including the coefficients of determination for calibration (R^2c) and cross-validation (R^2v), the root means square error of calibration (RMSEC), the root means square error of cross-validation (RMSEV), and model bias [64]. The optimal model was selected based on the combination of high R^2c and R^2v values with minimal RMSEC, RMSEV, and bias. Furthermore, model predictive accuracy was quantified using standard performance metrics—coefficient of determination (R^2; Equation 1), RMSEV (Equation 2), and RMSEC (Equation 3)—which collectively assess the degree of agreement between predicted and reference values [2]. The equations used for these metrics are presented as follows:

Equation 1:

$$R^2 = \frac{\sum_{i=1}^{n}(\hat{y}\mathrm{i} - \mathrm{yi})^2}{\sum_{i=1}^{n}(\hat{y}\mathrm{i} - \mathrm{ym})^2}$$

Equation 2:

$$RMSEV = \sqrt{\frac{1}{\mathrm{nv} - 1}\sum_{i=1}^{nv}(\hat{y}\mathrm{i} - \mathrm{yi} - \mathrm{bias})^2}$$

Equation 3:

$$RMSEC = \sqrt{\frac{1}{\mathrm{nc} - 1}\sum_{i=1}^{nc}(\hat{y}\mathrm{i} - \mathrm{yi})^2}$$

Where - n as the total number of data samples, - nc as the count of calibration data samples, - nv as the count of validation data samples, - ŷi as the predicted value, - yi as the actual value, and - ym as the mean actual value. The average deviations between the predicted and actual values are noted as a potential bias (Equation 4).

Equation 4:

$$Bias = \frac{1}{\mathrm{nv}}\sum_{i=1}^{nv}(\hat{\mathrm{y}}\mathrm{i} - \mathrm{yi})$$

Model calibration involved 0–7 latent variables (LVs) as recommended by [52] and [57]. Lower RMSEC and RMSEV values indicated better model performance [5 & 63].

A regression model based on the Partial Least Squares (PLS) framework was employed to develop calibration and validation models for both rind and flesh colour metrics (L*, a*, b*, C*, ΔE, and h°) following the initial stage of spectral pretreatment. To ensure model reliability and minimize overfitting, a random cross-validation procedure was applied to the calibration dataset. The external validation dataset was subsequently used to evaluate the predictive performance of the established regression models.

The Root Mean Square Error of Calibration (RMSEC) was used as a measure of how accurately the calibration models could predict reference values within the calibration dataset. Lower RMSEC values indicate a higher degree of model accuracy and reduced prediction error [5 & 57]. Similarly, the Root Mean Square Error of Validation (RMSEV) was employed as a statistical index to evaluate model performance on the independent validation dataset during the second stage of pretreatment. RMSEV represents the average prediction error expected when the calibration model is applied to new, unseen samples for both rind and flesh colour metrics (L*, a*, b*, C*, ΔE, and h°) measurements.

In this study, the number of latent variables (LVs) used in the PLS models ranged from 0 to 7, following the recommendations of [52] and [57], who demonstrated that appropriate LV selection is essential for constructing robust and generalisable predictive models.

Here, *n* denotes the total number of samples, n_c and n_v represent the number of samples used for calibration and validation, respectively. The predicted value is expressed as $\hat{y}_i$, the corresponding measured (reference) value as y_i, and the mean of measured values as y_m. The average difference between predicted and reference values was calculated as bias (Equation 5), while the Residual Predictive Deviation (RPD) value (Equation 6) was determined to evaluate the predictive strength and stability of the PLS models.

Equation 5:

$$Bias = \frac{1}{\mathrm{nv}}\sum_{i=1}^{nv}(\hat{\mathrm{y}}\mathrm{i} - \mathrm{yi})$$

Equation 6:

$$RPD = \frac{\mathrm{SD}}{\mathrm{RMSEP}}$$

The experiment followed a completely randomised design (CRD) with three replicates. Analysis of variance (ANOVA) was performed to determine treatment effects, and mean comparisons were conducted using Fisher's Protected Least Significant Difference (LSD) test at $p \leq 0.05$. All statistical computations and correlation analyses were carried out in R software (version 4.0.4).

3. Result

3.1 Spectral Characteristics of Jackfruit Rind

Figures 1 and 2 present the unprocessed spectral reflectance profiles of healthy and bronzing-affected jackfruit samples at 12 weeks after anthesis (WAA), whereas Figures 3 and 4 display the corresponding preprocessed Vis–NIR spectra, derived from a total of 1,620 samples. In the Vis–NIR region, most absorption bands represent either overtones or combinations of fundamental absorption features in the infrared region, producing broad and overlapping peaks—a phenomenon frequently reported in fruits and vegetables [46].

The average absorption pattern, derived from thirty discrete portions of each jackfruit sample, revealed distinct spectral characteristics across the rind's latitudinal zones. To assess spatial spectral variability, the rind was systematically segmented into five layers: top (A1–A6), middle-top (B1–B6), middle (C1–C6), middle-bottom (D1–D6), and bottom (E1–E6). Broad absorption patterns in the Vis–NIR range were attributed to overlapping signals from complex molecular vibrations, combination bands, and overtones of spectrally active functional groups. Both healthy and bronzing-affected fruits exhibited pronounced absorption peaks near 675 nm and 945 nm. A notable absorption feature was also observed around 970 nm, consistent with the second overtone of water reported in apples [45]. Spectral features between 940 nm and 970 nm may additionally be linked to sucrose content, as indicated in passion fruit [39], whereas a minor absorption at 970 nm could be associated with fructose presence, corroborating findings in canned tender jackfruit [9]. Collectively, these results highlight the influence of water- and sugar-related compounds on the Vis–NIR spectral response of jackfruit rind and confirm the presence of chemically meaningful absorption patterns relevant to fruit physiology and postharvest quality assessment.

The unprocessed spectrum for healthy jackfruit at 12 WAA is shown in Figure 4, while Figure 5 depicts the corresponding spectrum for bronzing-affected rind. These raw spectra illustrate scattering effects and baseline shifts. After preprocessing using the Savitzky–Golay smoothing and standard normal variate (SNV) correction methods, the spectra for normal and bronzing fruits are shown in Figures 6 and 7, respectively. In these pretreated spectra, significant absorption is evident in the 500–950 nm range, with distinct peaks at 760 nm and 970 nm, similar to those reported in durian pulp [57] (Saechua *et al*., 2021). The absorption at 760 nm corresponds to the third overtone of O–H stretching, while the 970 nm peak represents the second overtone of O–H stretching in water molecules [50].

Comparison of PLSR models derived from two scanning orientations revealed superior predictive performance when scanning was performed across all five latitudinal rind layers, with each layer divided into six portions (30 positions in total). The detailed performance metrics of PLSR models for predicting rind and flesh pH, as well as rind and flesh titratable acidity, across 10, 12, and 14 WAA in the 500–950 nm range, are presented in Tables 4–10. The optimal model employed moving average smoothing with a 12-segment combination, achieving the highest coefficients of determination and lowest root mean square errors for calibration, validation, and prediction datasets.

The regression coefficient plots for the best-performing PLSR models (Figures 5-28) illustrate the critical wavelength regions for predicting rind and flesh pH, as well as titratable acidity. Prominent regression peaks were identified within the 700–1100 nm range, with absorption features for water at 754 nm (shifted to 760 nm due to the third overtone of O–H stretching) and at 979 nm (shifted to 970 nm due to the third overtone of C–H stretching). These wavelength-specific absorptions reinforce the role of water and organic constituents in driving the Vis–NIR spectral responses of jackfruit rind.

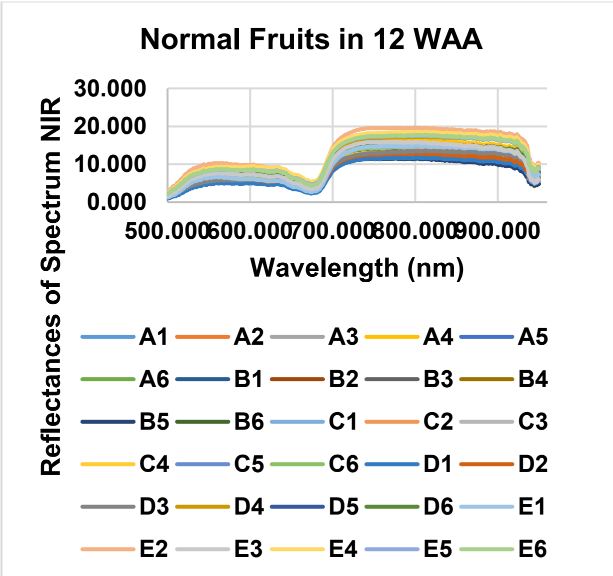

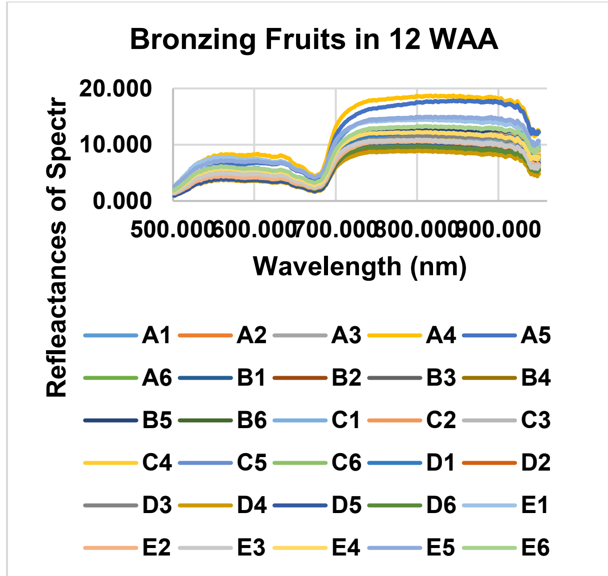

*The rind was systematically segmented into five layers—top (A1 to A6), middle-top (B1 to B6), middle (C1 to C6), middle-bottom (D1 to D6), and bottom (E1 to E6)—to assess spatial spectral variability.

Figure 1 (Left): Mean spectral reflectance of raw material for normal fruit of 30 portions in 12 WAA.

Figure 2 (Right): Mean spectral reflectance of raw material for bronzing fruit of 30 portions in 12 WAA.

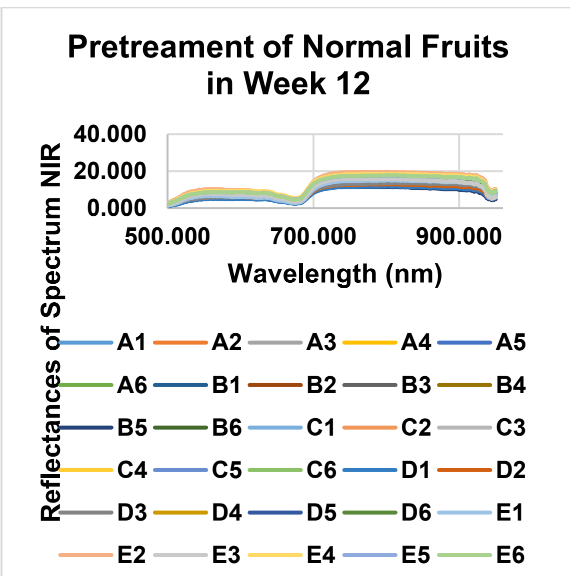

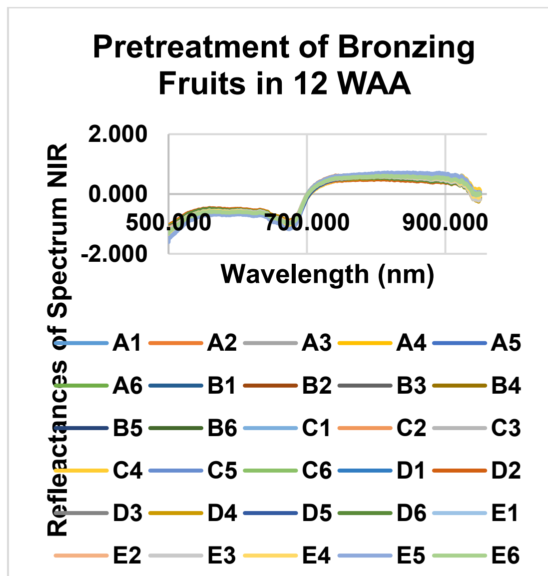

*The rind was systematically segmented into five layers—top (A1 to A6), middle-top (B1 to B6), middle (C1 to C6), middle-bottom (D1 to D6), and bottom (E1 to E6)—to assess spatial spectral variability.

Figure 3: Pre-treated mean spectrum Vis-NIR reflectance for normal fruit of 30 portions in 12 WAA using Savitzky-Golay and SNV preprocessed spectral.

Figure 4: Pre-treated mean spectrum Vis-NIR reflectance for bronzing fruit of 30 portions in 12 WAA using Savitzky-Golay and SNV preprocessed spectral.

3.2 Performance of PLSR calibration and prediction models using twelve pretreatments

*3.2.1 Predictive performance of PLSR models for rind colour L*at 10 WAA*

The outcomes of the partial least squares regression (PLSR) models for predicting jackfruit rind lightness (L*) from visible near-infrared (Vis-NIR) spectra (500–950 nm) demonstrated strong predictive capability under both normal and bronzed conditions. As presented in Table 1 and Figures 5–6, the optimal spectral pretreatment for Week 10 maturity was achieved using a combination of Savitzky–Golay smoothing and standard normal variate (SNV) correction, employing seven latent variables (LVs).

For normal jackfruit rind, the calibration model yielded a coefficient of determination (Rc^2) of 0.95 and a root mean square error of calibration (RMSEc) of 0.29, with the regression equation $y = 0.947x + 0.143$. The prediction model achieved an Rp^2 of 0.92 and RMSEp of 0.37 ($y = 0.911x + 0.205$), as shown in Figure 5. The corresponding residual prediction deviation (RPD) value of 16.19 indicates excellent predictive performance, as RPD values greater than 3 are generally considered good, while values exceeding 5 denote outstanding model robustness and reliability for quantitative prediction.

For bronzed jackfruit rind**,** the optimal configuration similarly involved Savitzky–Golay + SNV preprocessing with seven LVs. The calibration model achieved $Rc^2 = 0.95$ and RMSEc = 0.34 ($y = 0.946x + 0.105$), while the prediction model produced $Rp^2 = 0.90$ and RMSEp = 0.43 ($y = 0.884x + 0.271$), as depicted in Figure 6. The corresponding RPD value of 6.66 also reflects a strong predictive model, suitable for reliable quantitative applications.

Across maturity stages (10–14 WAA), RPD values ranged from 6.60 to 16.19 for normal fruits and 6.66 to 13.62 for bronzed fruits, confirming the robustness and generalizability of the PLSR models in estimating rind colour lightness across different physiological conditions. Overall, these findings underscore the effectiveness of Vis-NIR spectroscopy combined with appropriate spectral pretreatment and PLSR modeling for non-destructive evaluation of jackfruit rind lightness (*Artocarpus heterophyllus* cv. Tekam Yellow), particularly at Week 10 maturity when the predictive models demonstrated the highest accuracy and stability.

Table 1: Summary of principal results obtained in the PLS models effects of fruit condition and maturity stages (weeks after anthesis) on rind colour L* of jackfruit cv. Tekam Yellow.

H	WAA	Mean	SD	Rc^2	RMSEc	Rp^2	RMSEp	Bias	Slope	Offset	Cor	RPD
N	10	36.61a	2.83	0.95	0.29	0.92	0.37	-0.02	0.91	0.20	0.96	16.19
B	10	33.05c	6.01	0.95	0.34	0.90	0.43	0.05	0.88	0.27	0.95	6.66
N	12	35.14b	5.17	0.94	0.37	0.91	0.43	0.04	0.89	0.18	0.96	8.69
B	12	36.08ab	3.75	0.93	0.40	0.93	0.37	-0.01	0.91	0.17	0.97	13.95
N	14	31.53d	6.09	0.91	0.37	0.79	0.57	0.04	0.85	0.26	0.89	6.60
B	14	33.28c	3.75	0.89	0.32	0.80	0.45	-0.10	0.85	0.16	0.90	13.62

H = Fruit condition, N = Normal, B = Bronzing, WAA = week after anthesis, SD = standard deviation, Cor = correlation, RPD = residual prediction deviation.

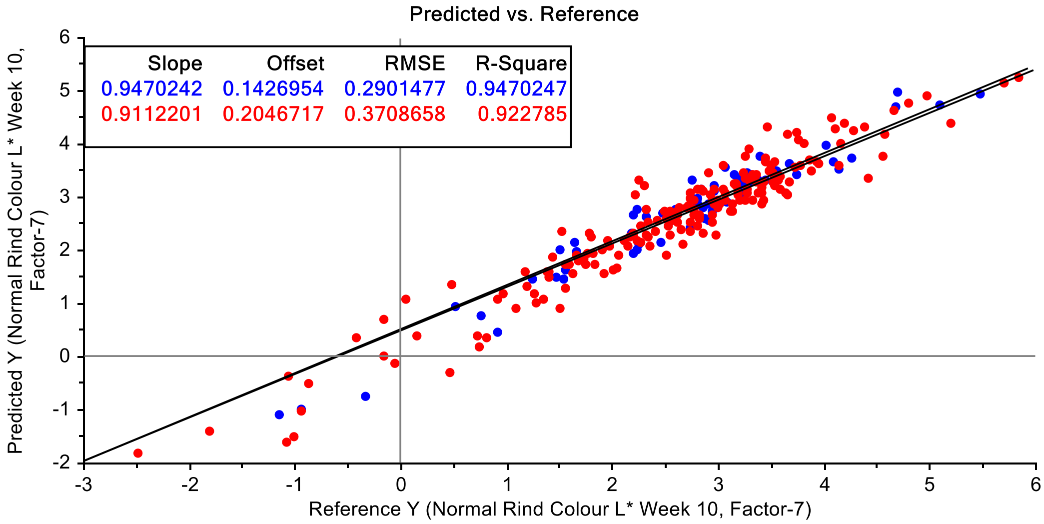

Figure 5: Scatter plots of referenced versus predicted normal rind colour L* in 10 WAA using reflectance spectral data with calibration model and prediction model. *• = Calibration Model, • = Prediction Model

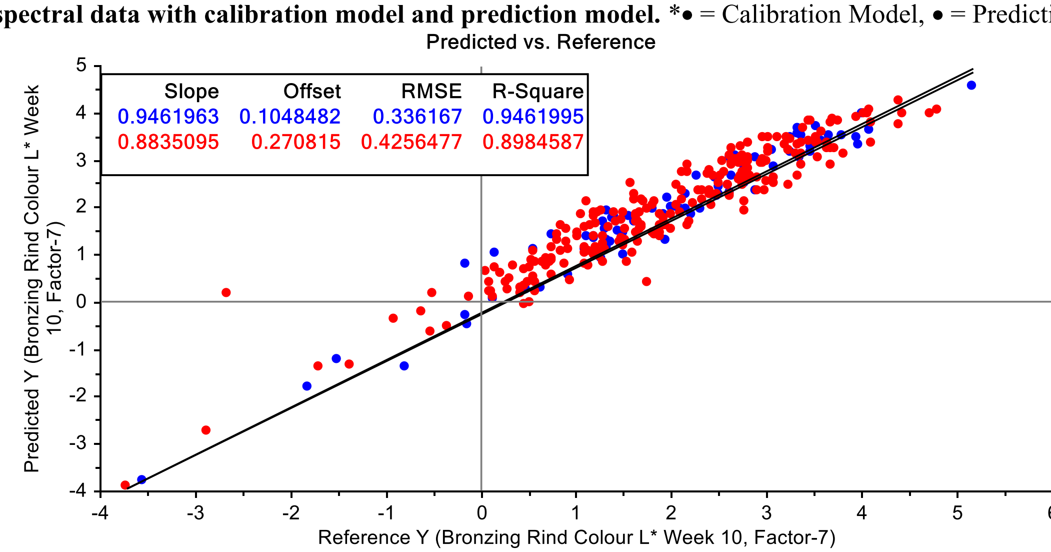

Figure 6: Scatter plots of referenced versus predicted bronzing rind colour L* in 10 WAA using reflectance spectral data with calibration model and prediction model. *• = Calibration Model, • = Prediction Model

3.2.2 Predictive performance of PLSR models for flesh colour L at 10 WAA*

The calibration and prediction outcomes using partial least squares regression (PLSR) within the 500–950 nm reflectance spectrum demonstrated strong predictive capability for jackfruit flesh lightness (L*) at Week 10. As summarised in Table 2 and Figure 7, the optimal spectral pretreatment for predicting normal (non-bronzed) jackfruit flesh colour was the combination of standard normal variate (SNV) and multiplicative scatter correction (MSC), using seven latent variables (LVs). The calibration model achieved high accuracy, with Rc^2 = 0.98 and *RMSEc* = 0.42, and the regression equation $y = 0.9808x + 0.3466$. The prediction model also exhibited excellent performance, yielding Rp^2 = 0.98 and *RMSEp* = 0.38, described by $y = 0.972x + 0.5188$.

The residual prediction deviation (RPD) value of 10.88 confirms the exceptional predictive power of this model. According to [66], RPD values greater than 3 indicate good quantitative prediction, while values exceeding 5 represent highly reliable and robust models suitable for analytical applications. Thus, the high RPD suggests that the PLSR model accurately characterises spectral variations corresponding to changes in jackfruit flesh colour lightness under normal conditions.

For bronzed jackfruit flesh at Week 10, the most effective pretreatment involved Savitzky–Golay smoothing combined with SNV, also with seven LVs (Table 2; Figure 8). The calibration model achieved Rc^2 = 0.96 and *RMSEc* = 0.44 ($y = 0.9581x + 0.3339$), whereas the prediction model yielded Rp^2 = 0.92 and *RMSEp* = 0.62 ($y = 0.9698x + 0.2404$). The associated RPD value of 16.21 demonstrates outstanding model performance, reflecting a high level of precision and stability even under physiological stress conditions that cause bronzing.

Across both fruit conditions and maturity stages (10–12 WAA), RPD values ranged between 10.73 and 16.21, signifying that all PLSR models developed for jackfruit flesh L* are highly reliable for quantitative assessment. These results underscore the potential of Vis–NIR spectroscopy, when coupled with appropriate spectral pretreatments and latent variable optimisation, to non-destructively and accurately predict flesh colour lightness (L)* of jackfruit (*Artocarpus heterophyllus* cv. Tekam Yellow) across different physiological states.

Table 2: Summary of principal results obtained in the PLS models effects of fruit condition and maturity stages (weeks after anthesis) on flesh colour L* of jackfruit cv. Tekam Yellow.

H	WAA	Mean	SD	Rc²	RMSEc	Rp²	RMSEp	Bias	Slope	Offset	Cor	RPD
N	10	81.84a	4.12	0.98	0.42	0.98	0.38	0.00	0.97	0.52	0.99	10.88
B	10	76.43bc	10.02	0.96	0.44	0.92	0.62	0.01	0.97	0.24	0.96	16.21
N	12	77.80b	8.81	0.94	0.72	0.93	0.81	0.00	0.95	0.31	0.96	10.84
B	12	75.51c	6.72	0.97	0.91	0.95	0.63	0.12	0.98	0.26	0.98	10.73

H = Fruit condition, N = Normal, B = Bronzing, WAA = week after anthesis, SD = standard deviation, Cor = correlation, RPD = residual prediction deviation.

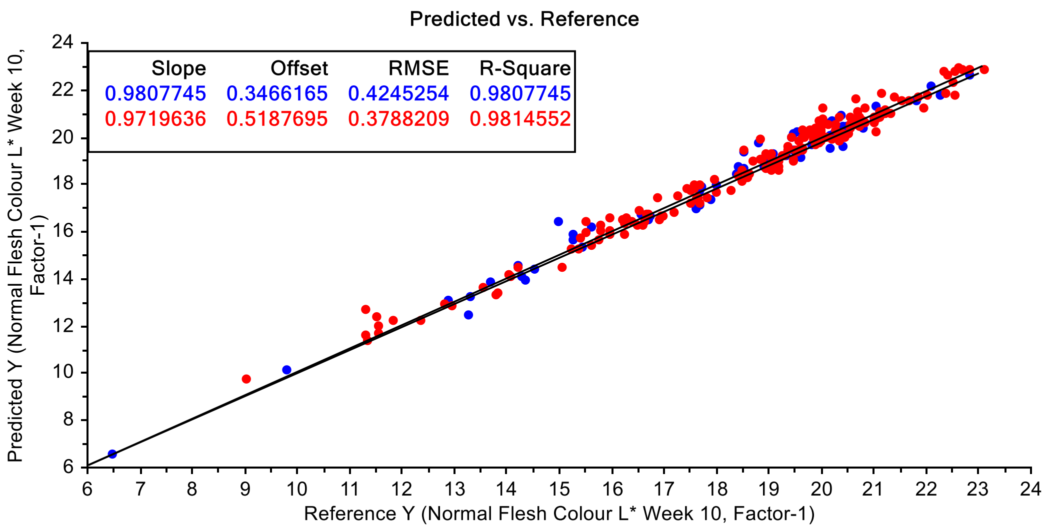

Figure 7: Scatter plots of referenced versus predicted normal flesh clour L* in 10 WAA using reflectance spectral data with calibration model and prediction model. *• = Calibration Model, • = Prediction Model

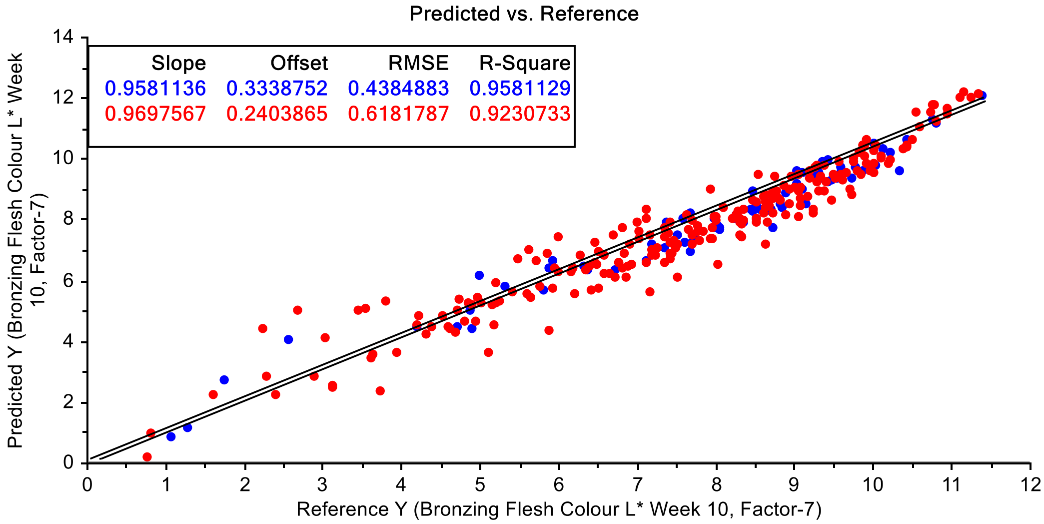

Figure 8: Scatter plots of referenced versus predicted bronzing flesh colour L* in Week 10 using reflectance spectral data with calibration model and prediction model. *• = Calibration Model, • = Prediction Model

3.2.3 Predictive performance of PLSR models for rind colour a* at 12 WAA

The calibration and prediction models using partial least squares regression (PLSR) within the 500–950 nm spectral range demonstrated a strong capability for predicting jackfruit rind colour a* at Week 12. As presented in Table 3 and Figure 9, the optimal spectral pretreatment for normal jackfruit rind was the combination of Savitzky–Golay smoothing and standard normal variate (SNV), employing seven latent variables (LVs). The calibration model yielded a coefficient of determination (Rc^2) of 0.93 and a root mean square error of calibration (*RMSEc*) of 0.46, described by the regression equation $y = 0.9296x + 0.1236$. The corresponding prediction model achieved Rp^2 = 0.88 and *RMSEp* = 0.58, with $y = 0.859x + 0.3018$.

The residual prediction deviation (RPD) value for this model was 4.74, indicating good quantitative predictive ability. According to established interpretative criteria (Williams & Norris, 2001; Fearn, 2002), RPD values between 3 and 5 denote models suitable for reliable screening and quantitative estimation, while values exceeding 5 represent highly accurate predictive performance. Thus, the model for normal rind a* demonstrates sufficient robustness for analytical evaluation of colour attributes using Vis–NIR data.

For bronzed jackfruit rind colour a*, the best-performing pretreatment was also Savitzky–Golay combined with SNV, using five LVs (Table 3; Figure 10). The calibration model achieved Rc^2 = 0.92 and *RMSEc* = 0.48 ($y = 0.9171x + 0.2260$), while the prediction model recorded Rp^2 = 0.92 and *RMSEp* = 0.47 ($y = 0.8913x + 0.2726$). The corresponding RPD value of 7.04 signifies excellent predictive accuracy, confirming that the PLSR model effectively captures the spectral variations associated with changes in red–green colour intensity under bronzing conditions.

Across different maturity stages (12–14 WAA), RPD values for rind a* prediction ranged from 4.65 to 8.91, indicating that all developed models exhibit good to excellent predictive performance. The higher RPD values obtained for bronzed samples suggest that spectral variation due to pigment degradation or physiological stress is well represented by the latent variable structure.

Overall, these results highlight that Vis–NIR spectroscopy, when combined with Savitzky–Golay + SNV preprocessing and optimised PLSR modelling, provides a reliable and non-destructive approach for estimating the a* colour parameter of jackfruit rind (*Artocarpus heterophyllus* cv. Tekam Yellow) at 12 WAA under both normal and bronzed conditions.

Table 3: Summary of principal results obtained in the PLS models effects of fruit condition and maturity stages (weeks after anthesis) on rind colour a* of jackfruit cv. Tekam Yellow.

H	WAA	Mean	SD	R_c^2	RMSEc	R_p^2	RMSEp	Bias	Slope	Offset	Cor	RPD
N	12	-1.04	2.73	0.93	0.46	0.88	0.58	0.06	0.86	0.30	0.94	4.74
B	12	-2.76	3.28	0.92	0.48	0.92	0.47	-0.02	0.89	0.27	0.96	7.04
N	14	-2.73	2.03	0.87	0.36	0.80	0.44	-0.01	0.83	-0.38	0.89	4.65
B	14	-1.13	4.27	0.91	0.41	0.87	0.48	-0.12	0.92	0.08	0.94	8.91

H = Fruit condition, N = Normal, B = Bronzing, WAA = week after anthesis, SD = standard deviation, Cor = correlation, RPD = residual prediction deviation.

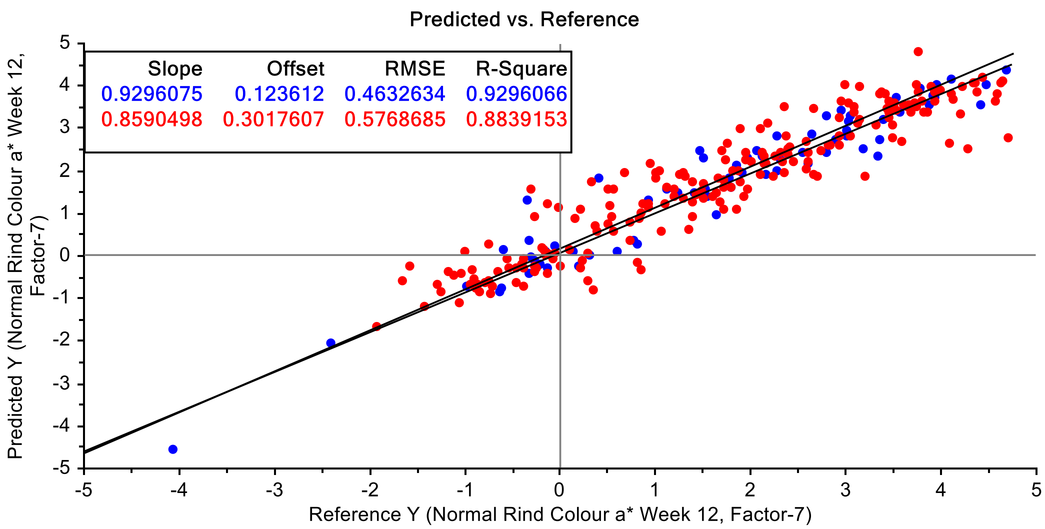

Figure 9: Scatter plots of referenced versus predicted normal rind colour a* in 12 WAA using reflectance spectral data with calibration model and prediction model. *• = Calibration Model, • = Prediction Model

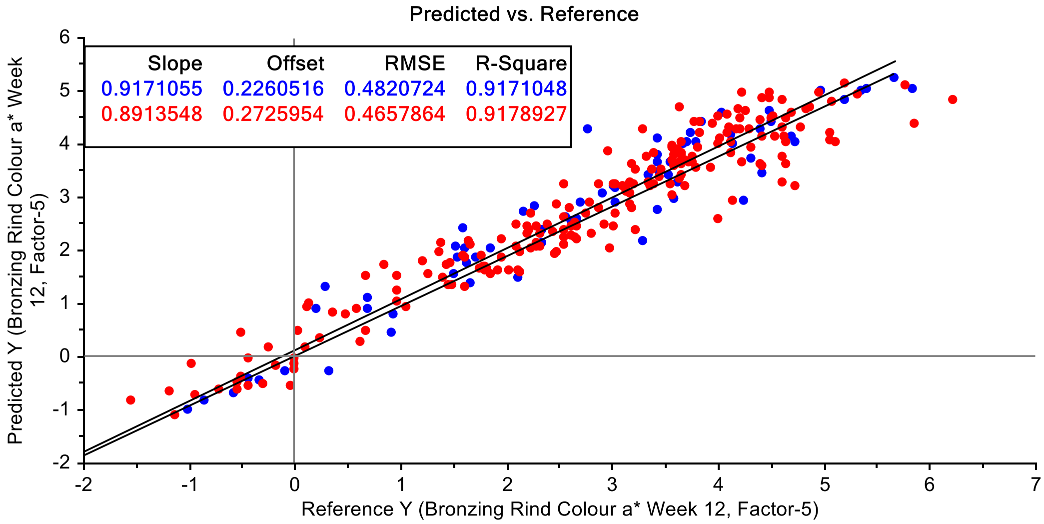

Figure 10: Scatter plots of referenced versus predicted bronzing rind colour a* in 12 WAA using reflectance spectral data with calibration model and prediction model. *• = Calibration Model, • = Prediction Model

3.2.4 Predictive performance of PLSR models for flesh colour a at 14 WAA*

The results of the calibration and prediction models using partial least squares regression (PLSR) within the 500–950 nm spectral range for jackfruit flesh indicate that the optimal pretreatment for predicting the a* colour value of normal jackfruit flesh in Week 14 was standard normal variate (SNV) and baseline correction, both with one latent variable (LV), as shown in Table 4 and Figure 11. The calibration model yielded a coefficient of determination $Rc^2 = 0.99$ and a root mean square error of calibration (RMSEc) of 0.84. The corresponding prediction model achieved $Rp^2 = 0.99$ and RMSEp = 0.98. The regression equations for the calibration and prediction models were $y = 0.9925x + 0.0302$ and $y = 0.9869x + 0.2724$, respectively. The residual prediction deviation (RPD) value of 2.31 indicates moderate predictive performance, suggesting that the model is suitable for approximate quantitative prediction of the flesh colour parameter in normal jackfruit.

In contrast, the optimal pretreatment for predicting the a* colour value of bronzed jackfruit flesh in Week 14, as presented in Table 4 and Figure 12, was identified as Savitzky–Golay smoothing combined with SNV, both with four LVs. The calibration model achieved $Rc^2 = 0.94$ and RMSEc = 0.61, while the prediction model recorded $Rp^2 = 0.90$ and RMSEp = 0.71. The corresponding calibration and prediction regression equations were $y = 0.9359x + 0.4965$ and $y = 0.9309x + 0.5540$, respectively. The RPD value of 3.13 indicates excellent model performance, confirming the strong predictive capability of the Vis–NIR model in estimating the a* colour value of bronzed jackfruit flesh.

These findings highlight the effectiveness of Vis–NIR spectroscopy, coupled with appropriate pretreatment strategies, in accurately predicting the a* colour parameter of jackfruit flesh under both normal and bronzed conditions during Week 14. The higher RPD value for bronzed flesh further demonstrates the model's robustness and potential application for nondestructive quality assessment in jackfruit postharvest analysis.

Table 4: Summary of principal results obtained in the PLS models effects of fruit condition and maturity stages (weeks after anthesis) on flesh colour a* of jackfruit cv. Tekam Yellow.

H	WAA	Mean	SD	Rc^2	RMSEc	Rp^2	RMSEp	Bias	Slope	Offset	Cor	RPD
N	**14**	**4.357a**	**2.26**	**0.99**	**0.84**	**0.99**	**0.98**	**0.21**	**0.99**	**0.27**	**1.00**	**2.31**

B	**14**	**2.576b**	**2.22**	**0.94**	**0.61**	**0.90**	**0.71**	**0.01**	**0.93**	**0.55**	**0.95**	**3.13**

H = Fruit condition, N = Normal, B = Bronzing, WAA = week after anthesis, SD = standard deviation, Cor = correlation, RPD = residual prediction deviation.

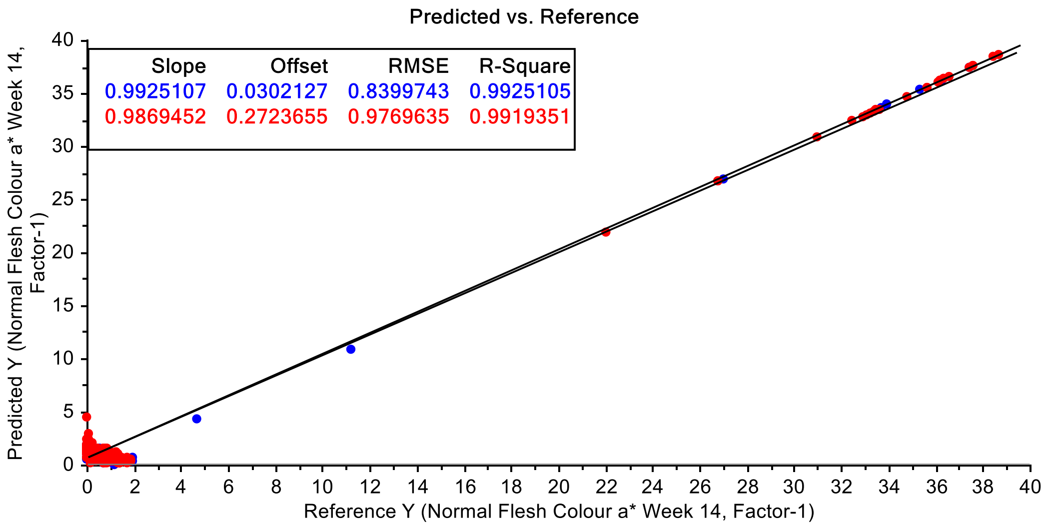

Figure 11: Scatter plots of referenced versus predicted normal flesh colour a* in 14 WAA using reflectance spectral data with calibration model and prediction model. *• = Calibration Model, • = Prediction Model

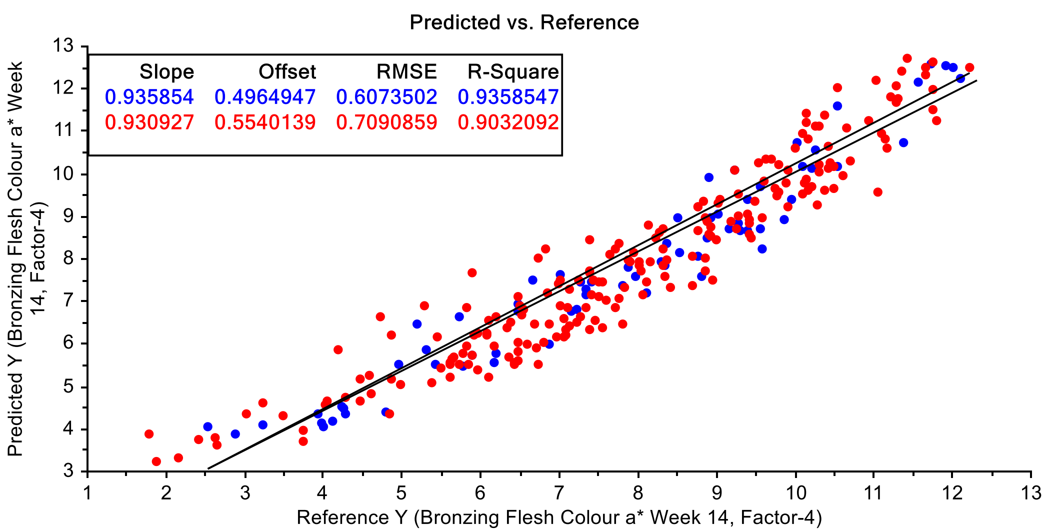

Figure 12: Scatter plots of referenced versus predicted bronzing flesh colour a* in 14 WAA using reflectance spectral data with calibration model and prediction model. *• = Calibration Model, • = Prediction Model

3.2.5 Predictive performance of PLSR models for rind colour b at 14 WAA*

The results from the calibration and prediction models using PLSR within the 500–950 nm spectral range indicate that the optimal pretreatment for predicting the **b*** colour value of normal jackfruit rind at Week 12 was the combination of Savitzky–Golay smoothing and standard normal variate (SNV), using seven latent variables (LVs), as shown in Table 5 and Figure 13. The calibration model achieved an $Rc^2 = 0.86$ and an RMSEc = 0.58, while the corresponding prediction model produced an $Rp^2 = 0.72$ and an RMSEp = 0.80. The regression equations for the calibration and prediction models were $y = 0.8589x + 0.0634$ and

$y = 0.7757x + 0.1306$, respectively. The residual prediction deviation (RPD) of 7.52 indicates excellent predictive performance, signifying that the model can reliably estimate the b* colour value of the normal rind with strong quantitative precision.

For bronzed jackfruit rind at Week 12, as presented in Table 5 and Figure 14, the same pretreatment (Savitzky–Golay + SNV, with seven LVs) was also identified as optimal. The calibration model recorded $Rc^2 = 0.89$ and RMSEc = 0.44, while the prediction model achieved $Rp^2 = 0.87$ and RMSEp = 0.50. The regression equations were $y = 0.891x + 0.1741$ (calibration) and $y = 0.8562x + 0.2682$ (prediction). The RPD value of 11.49 indicates outstanding predictive capability, confirming the model's robustness and suitability for accurate quantitative prediction of rind colour in bronzed jackfruit.

The high RPD values observed for both normal and bronzed rind models (RPD > 7) suggest excellent predictive precision, far exceeding the minimum threshold (RPD ≥ 3.0) typically required for reliable analytical use. These results underscore the potential of Vis–NIR spectroscopy, when paired with suitable pretreatment strategies, as a non-destructive and highly accurate tool for assessing rind colour variations in jackfruit across different fruit conditions at 14 WAA.

Table 5: Summary of principal results obtained in the PLS models effects of fruit condition and maturity stages (weeks after anthesis) on rind colour b* of jackfruit cv. Tekam Yellow.

H	WAA	Mean	SD	Rc^2	RMSEc	Rp^2	RMSEp	Bias	Slope	Offset	Cor	RPD
N	10	22.85a	5.70	0.92	0.42	0.79	0.70	0.05	0.74	0.65	0.89	8.15
B	10	20.80b	6.50	0.91	0.45	0.85	0.58	0.06	0.79	0.42	0.92	11.13
N	12	15.30c	6.05	0.86	0.58	0.72	0.80	0.03	0.78	0.13	0.85	7.52
B	12	20.98b	5.70	0.89	0.44	0.87	0.50	0.04	0.86	0.27	0.93	11.49
N	14	23.00a	6.96	0.88	0.62	0.65	1.03	0.09	0.80	0.79	0.82	6.74
B	14	19.64b	8.82	0.90	0.56	0.88	0.59	-0.11	0.93	-0.01	0.94	14.93

H = Fruit condition, N = Normal, B = Bronzing, WAA = week after anthesis, SD = standard deviation, Cor = correlation, RPD = residual prediction deviation.

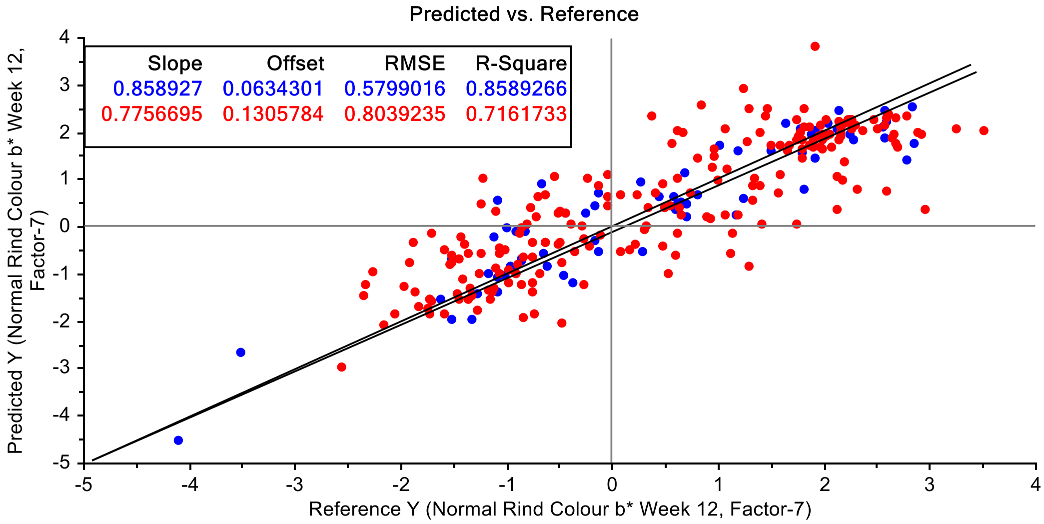

Figure 13: Scatter plots of referenced versus predicted normal rind colour b* in 14 WAA using reflectance spectral data with calibration model and prediction model. *• = Calibration Model, • = Prediction Model

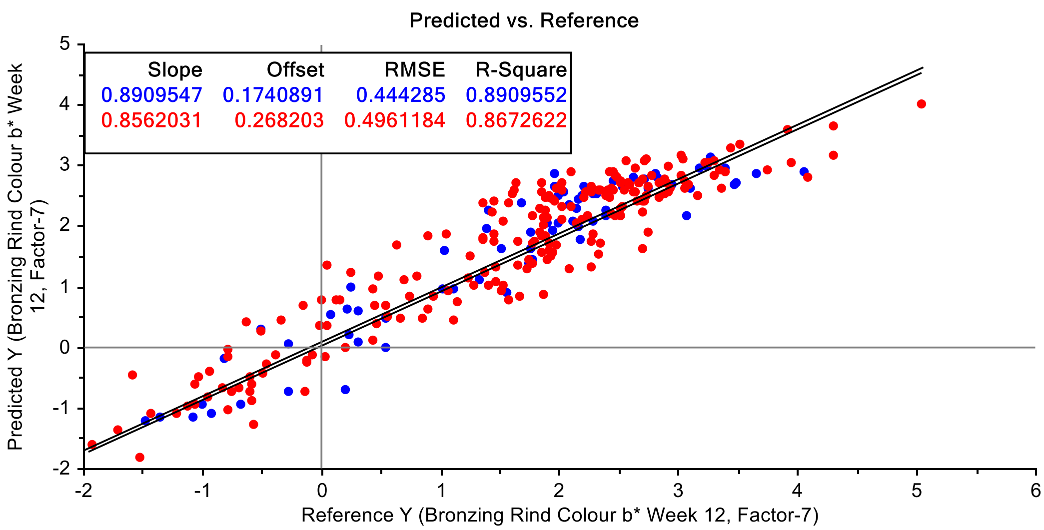

Figure 14: Scatter plots of referenced versus predicted bronzing rind colour b* in 14 WAA using reflectance spectral data with calibration model and prediction model. *• = Calibration Model, • = Prediction Model

3.2.6 Predictive performance of PLSR models flesh colour b at 14 WAA*

The outcomes of the calibration and prediction models using partial least squares regression (PLSR) within the 500–950 nm spectral range demonstrate that the most effective pretreatment method for predicting the b* colour value of normal jackfruit flesh at Week 14 was the Savitzky–Golay smoothing method with five latent variables (LVs). As shown in Table 6 and Figure 15, the calibration model achieved a coefficient of determination (Rc^2) of 0.83 and a root mean square error of calibration (RMSEc) of 1.05, with the regression equation $y = 0.8331x + 0.7870$. The prediction model yielded an Rp^2 of 0.76 and an RMSEp of 1.24, with the regression equation $y = 0.8051x + 0.8840$. The residual prediction deviation (RPD) value of 6.33 indicates excellent predictive performance, demonstrating that the model can accurately predict the b* colour parameter of the normal jackfruit flesh.

Similarly, for bronzed jackfruit flesh at Week 14, the Savitzky–Golay method with five LVs also provided the most effective pretreatment, as presented in Table 6 and Figure 16. The calibration model recorded an Rc^2 of 0.87 and RMSEc of 0.71, while the prediction model achieved an Rp^2 of 0.82 and RMSEp of 0.80. The regression equations were $y = 0.8716x + 0.6165$ (calibration) and $y = 0.8600x + 0.5931$ (prediction). The corresponding RPD value of 6.81 confirms high model robustness and reliability, supporting its use for accurate non-destructive prediction of b* colour in bronzed jackfruit flesh.

Overall, the high RPD values obtained for both normal (RPD = 6.33) and bronzed (RPD = 6.81) jackfruit flesh at Week 14 indicate excellent model performance, as RPD values greater than 3.0 generally represent strong predictive accuracy suitable for quantitative analysis. These findings affirm the robust potential of Vis–NIR spectroscopy, in combination with suitable pretreatment strategies and PLSR modeling, for effectively evaluating jackfruit flesh colour (b*) across varying fruit conditions at advanced maturity stages.

Table 6: Summary of principal results obtained in the PLS models effects of fruit condition and maturity stages (weeks after anthesis) on flesh colour b* of jackfruit cv. Tekam Yellow.

H	WAA	Mean	SD	Rc^2	RMSEc	Rp^2	RMSEp	Bias	Slope	Offset	Cor	RPD
N	10	35.781cd	3.87	0.94	0.42	0.86	0.64	0.03	0.80	1.09	0.93	6.08
B	10	30.939e	7.04	0.92	0.54	0.80	0.82	-0.09	0.92	0.26	0.90	8.58
N	12	37.624ab	4.49	0.93	0.60	0.89	0.76	0.02	0.93	0.28	0.95	5.95
B	12	35.213d	5.92	0.92	0.66	0.91	0.74	0.05	0.91	0.42	0.95	8.04
N	14	38.87a	7.84	0.83	1.05	0.76	1.24	0.07	0.81	0.88	0.87	6.33
B	14	37.178bc	5.43	0.87	0.71	0.82	0.80	-0.10	0.86	0.59	0.91	6.81

H = Fruit condition, N = Normal, B = Bronzing, WAA = week after anthesis, SD = standard deviation, Cor = correlation, RPD = residual prediction deviation.

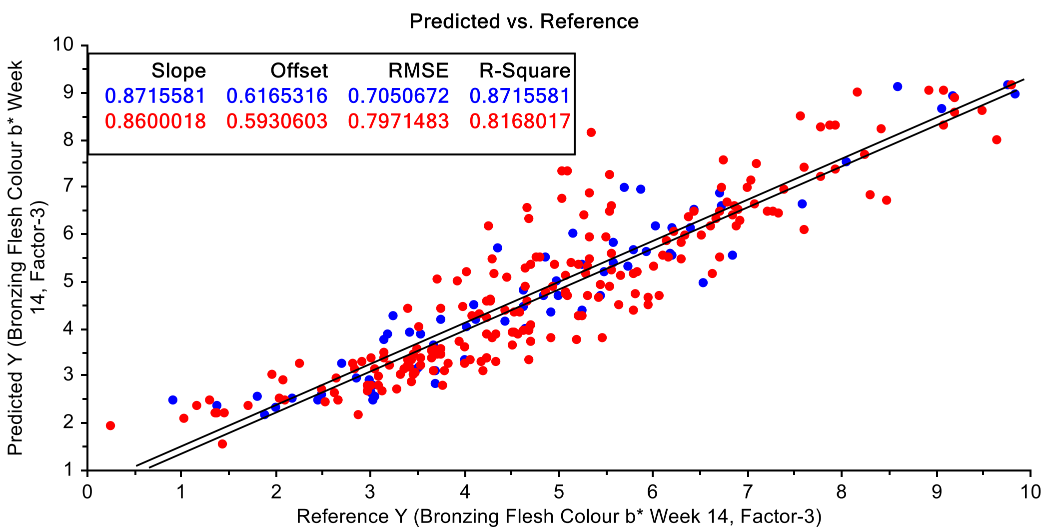

Figure 15: Scatter plots of referenced versus predicted normal flesh colour b* in 14 WAA using reflectance spectral data with calibration model and prediction model. *• = Calibration Model, • = Prediction Model

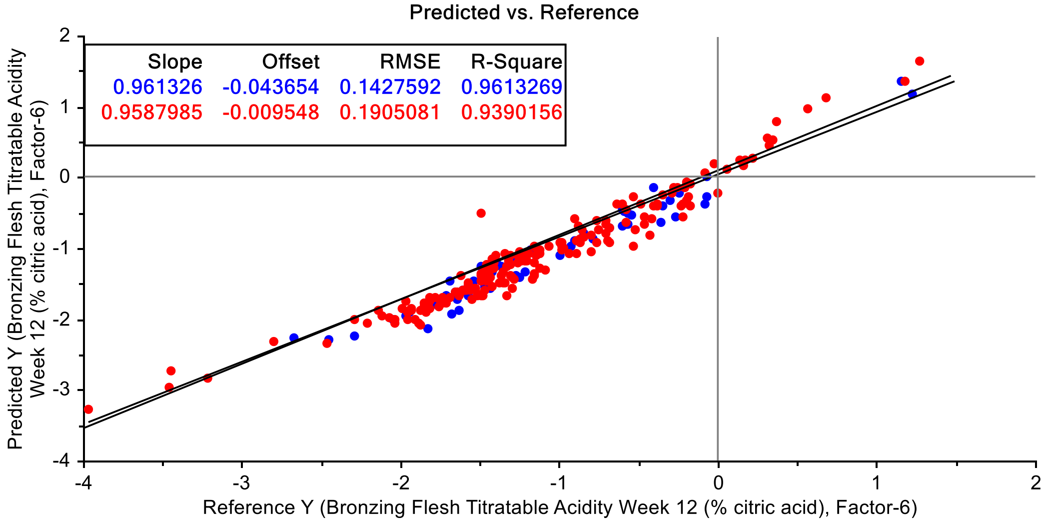

Figure 16: Scatter plots of referenced versus predicted bronzing flesh colour b* in 14 WAA using reflectance spectral data with calibration model and prediction model. *• = Calibration Model, • = Prediction Model

3.2.7 Predictive performance of PLSR models rind colour C at 10 WAA*

The calibration and prediction results obtained using partial least squares regression (PLSR) within the 500–950 nm spectral range reveal that the optimal spectral pretreatment for predicting the chroma (C*) value of normal jackfruit rind at Week 10 was the combination of Savitzky–Golay smoothing and standard normal variate (SNV) transformation, utilizing six latent variables (LVs). As presented in Table 7 and Figure 17, the calibration model achieved a coefficient of determination (Rc^2) of 0.95 and a root mean square error of calibration (RMSEc) of 0.42, with the regression equation $y = 0.9475x + 0.4025$. The corresponding prediction model yielded an Rp^2 of 0.94 and RMSEp of 0.54, with the equation $y = 0.8692x + 0.9718$. The residual prediction deviation (RPD) value of 12.14 indicates excellent predictive capability, confirming that the PLSR model effectively predicts rind chroma (C*) under normal fruit conditions at Week 10.

For bronzed jackfruit rind, the same pretreatment combination (Savitzky–Golay and SNV with six LVs) also produced optimal results, as shown in Table 7 and Figure 18. The calibration model achieved an Rc^2 of 0.95 and RMSEc of 0.54, while the prediction model reached an Rp^2 of 0.92 and RMSEp of 0.60. The corresponding regression equations were $y = 0.9511x + 0.3270$ for calibration and $y = 0.9256x + 0.4956$ for prediction. The RPD value of 9.92 further supports the model's strong predictive performance, demonstrating its reliability for quantifying rind chroma in bronzed jackfruit.

Overall, both normal and bronzed rind samples exhibited high R^2 values (≥ 0.92), low RMSEs, and RPD values exceeding 9.0, all of which are indicative of excellent model performance and predictive reliability. Since RPD values greater than 3.0 are generally considered suitable for quantitative prediction, the exceptionally high RPD values in this study confirm that the Vis–NIR spectral data, combined with appropriate pretreatment and PLSR modeling, can provide robust, non-destructive predictions of rind chroma (C*) at the early maturity stage (10 WAA).

Table 7: Summary of principal results obtained in the PLS models effects of fruit condition and maturity stages (weeks after anthesis) on rind colour C* of jackfruit cv. Tekam Yellow.

H	WAA	Mean	SD	Rc^2	RMSEc	Rp^2	RMSEp	Bias	Slope	Offset	Cor	RPD

N	**10**	**23.12a**	**5.94**	**0.95**	**0.42**	**0.94**	**0.54**	**0.00**	**0.87**	**0.97**	**0.97**	**12.14**
B	**10**	**21.13b**	**6.50**	**0.95**	**0.54**	**0.92**	**0.60**	**0.00**	**0.93**	**0.50**	**0.96**	**9.92**
N	**12**	**16.61c**	**6.02**	**0.96**	**0.58**	**0.87**	**0.97**	**0.08**	**0.88**	**0.61**	**0.93**	**5.72**
B	**12**	**21.43b**	**5.55**	**0.95**	**0.54**	**0.95**	**0.60**	**-0.03**	**0.96**	**0.18**	**0.97**	**9.99**
N	**14**	**23.44a**	**6.97**	**0.92**	**0.62**	**0.72**	**1.38**	**0.04**	**0.67**	**2.30**	**0.85**	**6.02**
B	**14**	**20.26b**	**8.31**	**0.85**	**0.87**	**0.83**	**0.90**	**-0.08**	**0.89**	**0.24**	**0.92**	**7.74**

H = Fruit condition, N = Normal, B = Bronzing, WAA = week after anthesis, SD = standard deviation, Cor = correlation, RPD = residual prediction deviation.

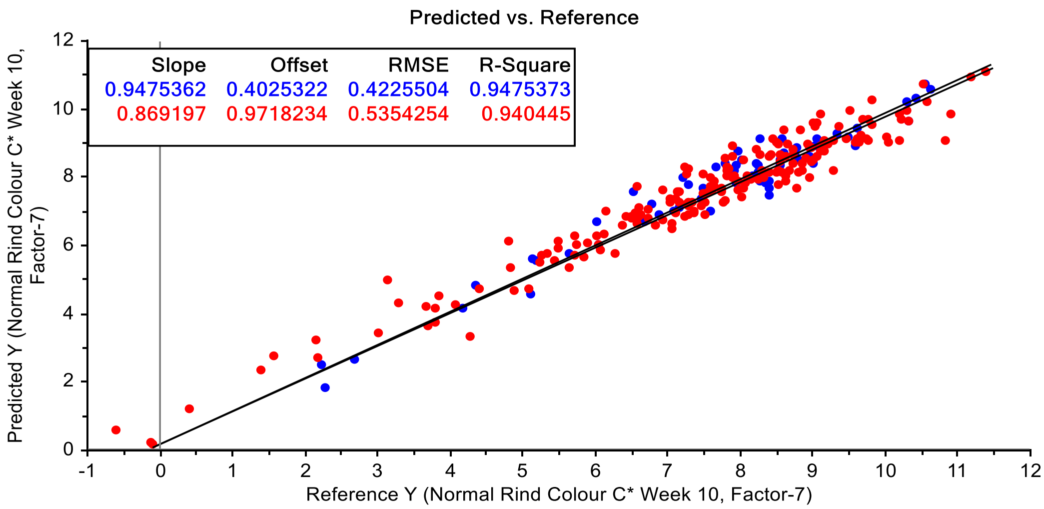

Figure 17: Scatter plots of referenced versus predicted normal rind colour C* in 10 WAA using reflectance spectral data with calibration model and prediction model. *• = Calibration Model, • = Prediction Model

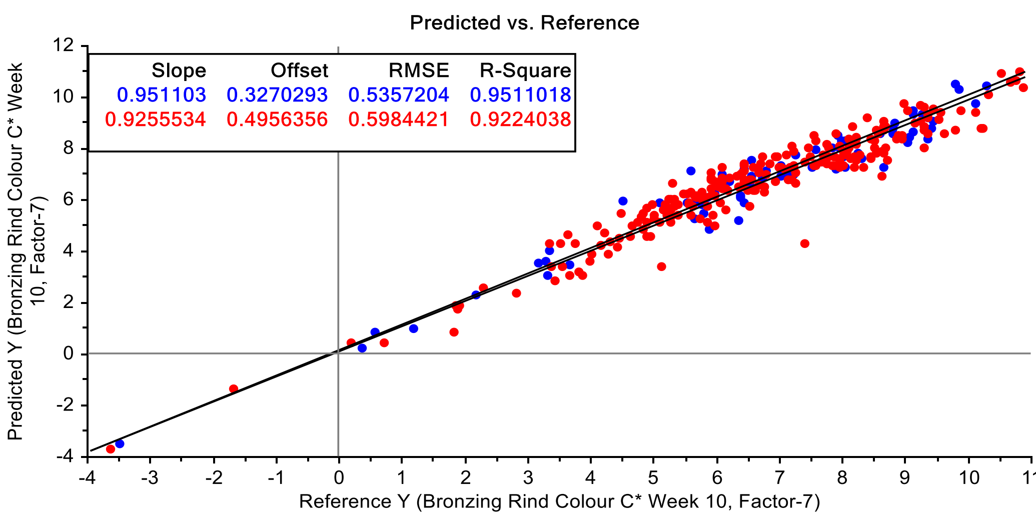

Figure 18: Scatter plots of referenced versus predicted bronzing rind colour C* in 10 WAA using reflectance spectral data for calibration model and prediction model. *• = Calibration Model, • = Prediction Model

3.2.8 Predictive performance of PLSR models flesh colour C at 10 WAA*

The results from the calibration and prediction models based on Partial Least Squares (PLS) regression, focusing on the spectral range of 500 to 950 nm, indicate that the most effective pretreatment technique for predicting the chroma (C*) value of the outer flesh of regular jackfruit at Week 10 was the combination of Savitzky-Golay smoothing and Standard Normal Variate (SNV), utilizing seven latent variables (LVs). As shown in Table 8 and Figure 19, the calibration model achieved a coefficient of determination (Rc^2) of 0.97 and a root mean square error of calibration (RMSEc) of 0.40, with the corresponding equation $y = 0.9706x + 0.2126$. The prediction model exhibited strong performance as well, with an Rp^2 of 0.93 and an RMSEp of 0.60, and the model equation $y = 0.9352x + 0.5665$.

For the bronzed jackfruit flesh at Week 10, the same pretreatment approach—Savitzky-Golay and SNV with seven LVs—was also identified as optimal. As presented in Table 8 and Figure 20, the calibration model achieved an Rc^2 of 0.90 and an RMSEc of 0.72, with the equation $y = 0.9036x + 0.6125$. The prediction model resulted in an Rp^2 of 0.82 and an RMSEp of 1.00, with the equation $y = 0.8426x + 0.8407$.

The Residual Prediction Deviation (RPD) values provide additional insight into model robustness. The RPD values of 6.20 for normal and 7.05 for bronzed jackfruit flesh indicate excellent predictive ability, as RPD values greater than 3.0 are generally considered to reflect models suitable for analytical applications, while values above 5.0 denote highly reliable quantitative prediction models. These high RPD values, coupled with strong Rc^2 and Rp^2 values (>0.90) and low RMSEp, demonstrate that the PLSR models achieved high precision and strong generalisation capability in predicting the chroma (C*) of jackfruit flesh at 10 WAA.

Overall, these findings underscore the potential of Vis-NIR spectroscopy, when combined with appropriate spectral pretreatments and PLS modeling, to accurately and non-destructively predict the chroma (C*) of jackfruit flesh at different colour stages.

Table 8: Summary of principal results obtained in the PLS models effects of fruit condition and maturity stages (weeks after anthesis) on flesh colour C* of jackfruit cv. Tekam Yellow.

H	WAA	Mean	SD	Rc^2	RMSEc	Rp^2	RMSEp	Bias	Slope	Offset	Cor	RPD
N	10	35.337c	3.73	0.97	0.40	0.93	0.60	0.07	0.94	0.57	0.96	6.20
B	10	31.850d	7.02	0.90	0.72	0.82	1.00	-0.14	0.84	0.84	0.91	7.05
N	12	37.669ab	4.55	0.95	0.62	0.93	0.75	0.05	0.95	0.34	0.96	6.09
B	12	35.133c	5.07	0.94	0.76	0.93	0.86	-0.03	0.96	0.21	0.96	5.88
N	14	39.126a	7.93	0.92	1.03	0.85	1.34	0.20	0.93	0.64	0.92	5.91
B	14	37.306b	5.51	0.90	0.90	0.89	0.93	-0.16	0.91	0.49	0.94	5.95

H = Fruit condition, N = Normal, B = Bronzing, WAA = week after anthesis, SD = standard deviation, Cor = correlation, RPD = residual prediction deviation.

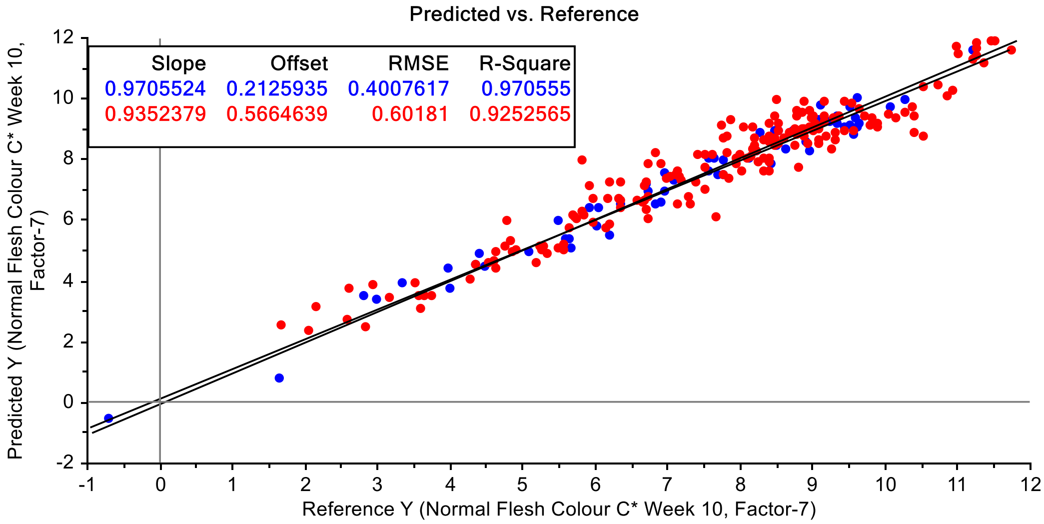

Figure 19: Scatter plots of referenced versus predicted normal flesh colour C* in Week 10 using reflectance spectral data with calibration model and prediction model. *• = Calibration Model, • = Prediction Model

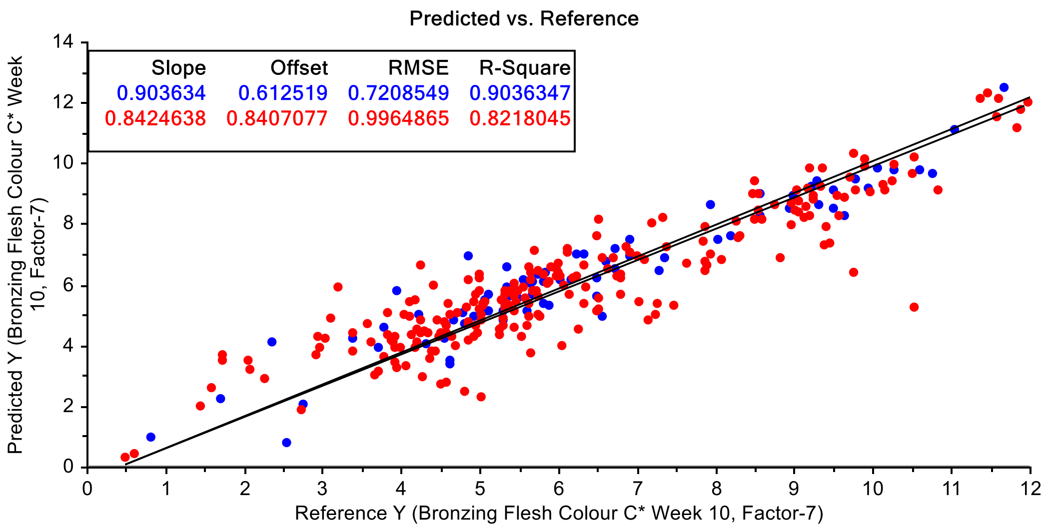

Figure 20: Scatter plots of referenced versus predicted bronzing flesh colour C* in Week 10 using reflectance spectral data with calibration model and prediction model. *• = Calibration Model, • = Prediction Model

3.2.9 Predictive performance of PLSR models rind colour ΔE at 12 WAA

The outcomes of the calibration and prediction models based on Partial Least Squares (PLS) regression within the spectral range of 500 to 950 nm reveal that the most effective pretreatment for predicting the colour difference (ΔE) of normal jackfruit rind at Week 12 was Standard Normal Variate (SNV) with seven latent variables (LVs). As presented in Table 9 and Figure 21, the calibration model yielded a coefficient of determination (Rc^2) of 0.92 and a root mean square error of calibration (RMSEc) of 1.12, with the regression equation $y = 0.9200x + 0.7181$. The corresponding prediction model produced an Rp^2 of 0.82 and an RMSEp of 1.60, with the equation $y = 0.8751x + 1.2147$.

For the bronzed appearance of the jackfruit rind at Week 12, the optimal pretreatment was a combination of SNV and Multiplicative Scatter Correction (MSC) with five LVs. As shown in Table 9 and Figure 22, the calibration model achieved an Rc^2 of 0.96 and an RMSEc of 0.69, with the model equation $y = 0.9612x + 0.3957$. The prediction model demonstrated high predictive accuracy, with an Rp^2 of 0.93 and an RMSEp of 0.88, and the corresponding equation $y = 0.9935x + 0.0082$.

The Residual Prediction Deviation (RPD) values further confirm the robustness of these models. The RPD value of 3.90 obtained for normal jackfruit rind indicates a good predictive model, suitable for screening or semi-quantitative applications. In contrast, the higher RPD value of 4.69 for bronzed rind reflects a strong quantitative predictive performance, as RPD values between 3.0 and 5.0 denote models with good to excellent prediction capability, while values above 5.0 indicate outstanding predictive reliability. These RPD results, coupled with high Rc^2 and Rp^2 values (≥ 0.90) and low prediction errors, highlight that the models effectively captured spectral variations associated with colour changes (ΔE) in the jackfruit rind at Week 12.

Collectively, these findings demonstrate that Vis-NIR spectroscopy, when combined with optimal pretreatments and PLSR modeling, provides a reliable non-destructive approach for monitoring rind colour evolution (ΔE) across different fruit conditions during the ripening process.

Table 9: Summary of principal results obtained in the PLS models effects of fruit condition and maturity stages (weeks after anthesis) on rind colour ΔE of jackfruit cv. Tekam Yellow.

H	WAA	Mean	SD	Rc^2	RMSEc	Rp^2	RMSEp	Bias	Slope	Offset	Cor	RPD
N	10	54.68bcd	6.57	0.97	0.45	0.91	0.87	-0.16	1.04	-0.63	0.96	7.42
B	10	53.84d	6.46	0.88	1.31	0.82	1.25	0.06	0.92	0.94	0.91	5.26
N	12	54.51cd	4.12	0.92	1.12	0.82	1.60	0.11	0.88	1.21	0.91	3.90
B	12	55.93bc	6.23	0.96	0.69	0.93	0.88	-0.06	0.99	0.01	0.97	4.69
N	14	59.42a	7.90	0.95	0.74	0.91	1.12	0.14	0.89	1.43	0.96	5.77
B	14	56.28b	6.47	0.94	0.94	0.89	1.28	0.12	0.89	1.33	0.94	6.16

H = Fruit condition, N = Normal, B = Bronzing, WAA = week after anthesis, SD = standard deviation, Cor = correlation, RPD = residual prediction deviation.

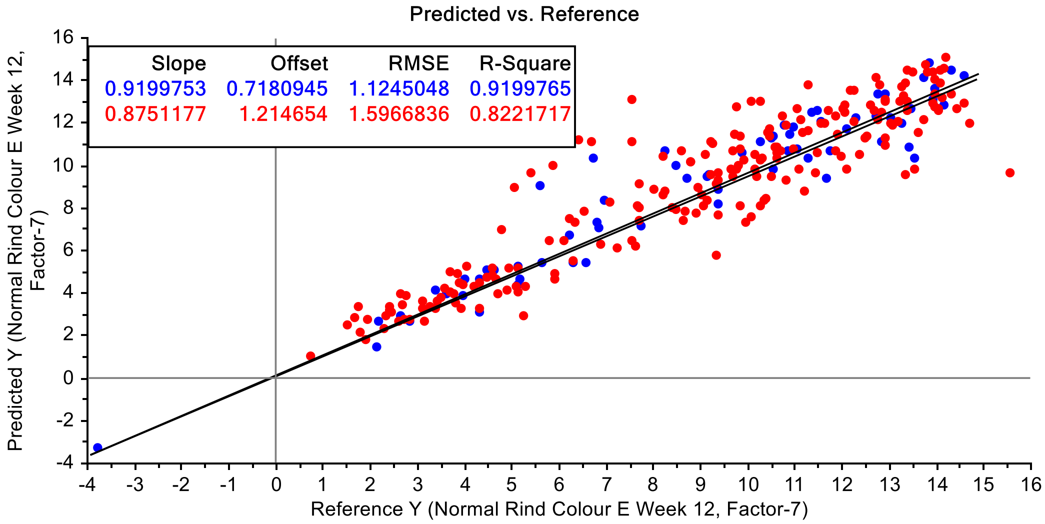

Figure 21: Scatter plots of referenced versus predicted normal rind colour ΔE in Week 12 using reflectance spectral data with calibration model and prediction model. *• = Calibration Model, • = Prediction Model

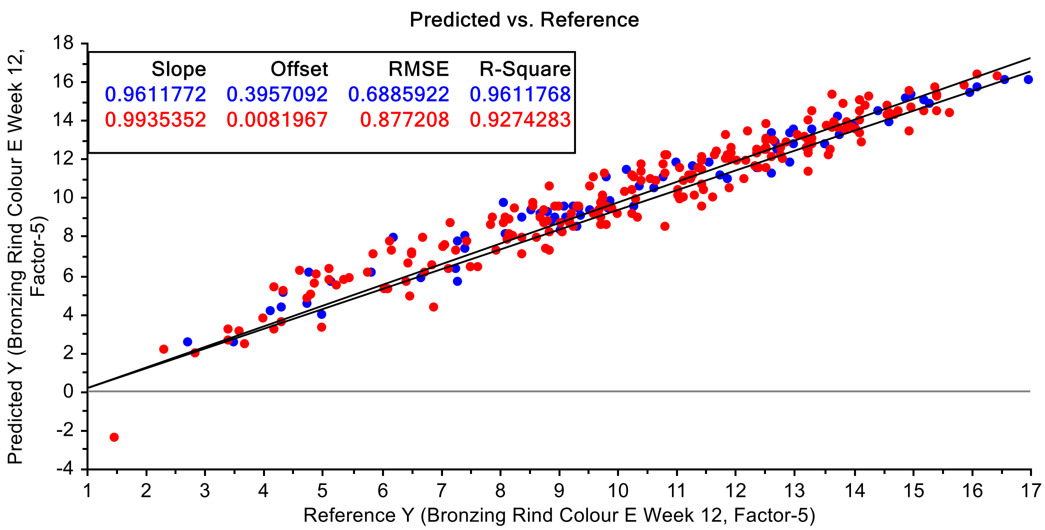

*• = Calibration Model, • = Prediction Model

Figure 22: Scatter plots of referenced versus predicted bronzing rind colour ΔE in Week 12 using reflectance spectral data with calibration model and prediction model.

3.2.10 Predictive performance of PLSR models flesh colour ΔE at 12 WAA

The outcomes from the calibration and prediction models based on the Partial Least Squares (PLS) regression approach within the visible–near infrared (Vis–NIR) spectral range (500–950 nm) indicate that the combination of Savitzky–Golay filtering and Standard Normal Variate (SNV) with five latent variables (LVs) was the most effective pretreatment for predicting the colour difference (ΔE) of normal jackfruit flesh at Week 12. As shown in Table 10 and Figure 23, the calibration model achieved a high coefficient of determination (Rc^2) of 0.98 and a low root mean square error of calibration (RMSEc) of 0.56, with the regression equation $y = 0.9819x + 0.1720$. The corresponding prediction model also demonstrated strong performance, with an Rp^2 of 0.98 and RMSEp of 0.59, and the regression equation $y = 0.9791x + 0.2010$.

For the bronzed flesh colour at Week 12, the optimal pretreatment was similarly achieved using Savitzky–Golay and SNV with four LVs. As illustrated in Table 10 and Figure 24, the calibration model yielded an Rc^2 of 0.98 and an RMSEc of 0.65, with the regression equation $y = 0.9758x + 0.2615$. The prediction model maintained high predictive accuracy, achieving an Rp^2 of 0.96 and an RMSEp of 0.80, with the corresponding equation $y = 0.9924x + 0.0204$.

The Residual Prediction Deviation (RPD) values substantiate the robustness of these PLSR models. The normal flesh model produced an RPD of 21.39, while the bronzed flesh model achieved an RPD of 16.04—both well above the threshold of 5.0, which indicates excellent quantitative predictive ability. Such high RPD values, coupled with Rc^2 and Rp^2 values exceeding 0.95 and minimal prediction errors, reflect exceptional model stability and reliability for predicting the flesh colour difference (ΔE) of jackfruit across varying physiological conditions.

Overall, these findings underscore that Vis–NIR spectroscopy, combined with appropriate spectral pretreatments and PLS regression, provides a powerful and non-destructive tool for accurately quantifying flesh colour variation (ΔE) in jackfruit cv. Tekam Yellow during the 12th week after anthesis.

Table 10: Summary of principal results obtained in the PLS models effects of fruit condition and maturity stages (weeks after anthesis) on flesh colour ΔE of jackfruit cv. Tekam Yellow.

H	WAA	Mean	SD	Rc^2	RMSEc	Rp^2	RMSEp	Bias	Slope	Offset	Cor	RPD
N	10	26.336bc	11.88	0.99	0.37	0.97	0.45	0.06	0.98	0.32	0.99	26.41
B	10	21.673d	12.26	0.92	0.69	0.90	0.93	-0.15	0.83	1.81	0.95	13.11
N	12	24.495cd	12.57	0.98	0.56	0.98	0.59	0.01	0.98	0.20	0.99	21.39
B	12	28.727b	12.81	0.98	0.65	0.96	0.80	-0.06	0.99	0.02	0.98	16.04
N	14	34.378a	11.65	0.97	0.85	0.95	1.06	0.12	1.02	-0.07	0.98	10.95
B	14	26.809bc	12.81	0.96	0.71	0.95	0.76	-0.09	0.95	0.49	0.97	16.96

H = Fruit condition, N = Normal, B = Bronzing, WAA = week after anthesis, SD = standard deviation, Cor = correlation, RPD = residual prediction deviation.

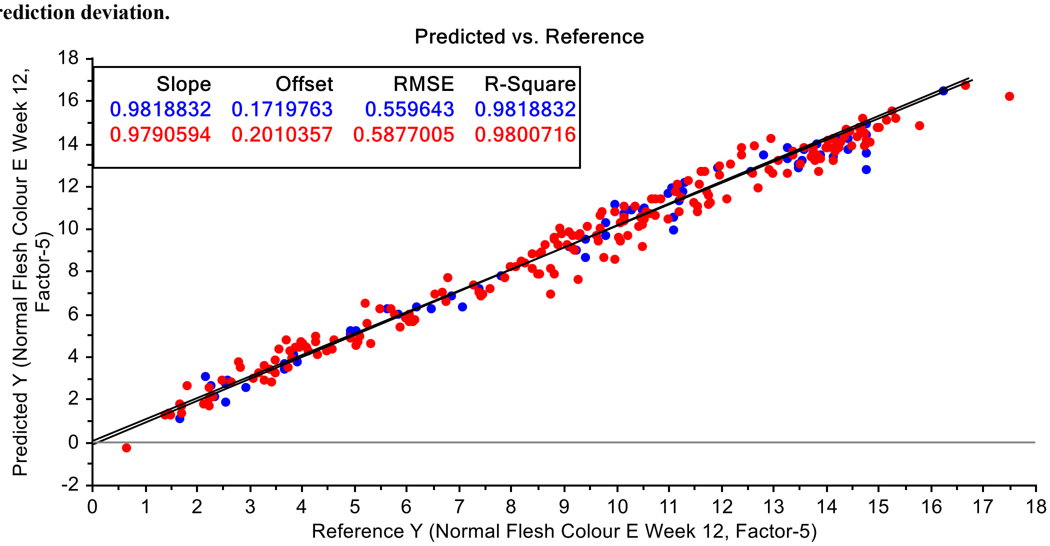

Figure 23: Scatter plots of referenced versus predicted normal flesh colour ΔE in Week 12 using reflectance spectral data with calibration model and prediction model. *• = Calibration Model, • = Prediction Model

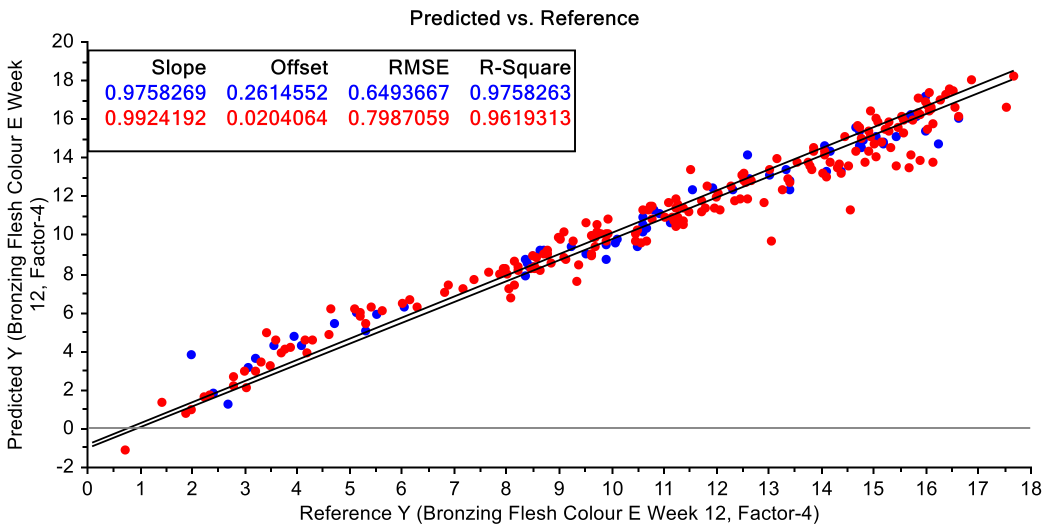

*• = Calibration Model, • = Prediction Model
Figure 24: Scatter plots of referenced versus predicted bronzing flesh colour ΔE in Week 12 using reflectance spectral data with calibration model and prediction model.

3.2.11 Predictive performance of PLSR models rind colour h° at 14 WAA

The outcomes of the calibration and prediction models based on Partial Least Squares (PLS) regression within the spectral range of 500–950 nm reveal that the combination of Standard Normal Variate (SNV) and Multiplicative Scatter Correction (MSC) with seven latent variables (LVs) was the most effective pretreatment for predicting the hue angle (h°) of normal jackfruit rind at Week 14. As presented in Table 11 and Figure 25, the calibration model achieved a high coefficient of determination (Rc^2) of 0.96 and a low root mean square error of calibration (RMSEc) of 0.69, with the regression equation $y = 0.9645x + 0.7072$. The corresponding prediction model yielded an Rp^2 of 0.90 and an RMSEp of 1.36, described by the equation $y = 0.9439x + 1.1162$.

For the bronzed jackfruit rind at Week 14, the optimal pretreatment method was identified as a combination of Savitzky–Golay smoothing and SNV. As shown in Table 11 and Figure 26, the calibration model achieved an Rc^2 of 0.94 and an RMSEc of 1.09, with the regression equation $y = 0.9367x + 0.8084$. The corresponding prediction model recorded an Rp^2 of 0.90 and an RMSEp of 1.37, with the regression equation $y = 0.9235x + 0.9579$.

The Residual Prediction Deviation (RPD) values further support the reliability of the models. The RPD value for the normal rind (RPD = 14.78) indicates excellent quantitative predictive capability, far exceeding the threshold of 3.0 typically regarded as suitable for robust predictive use. In contrast, the bronzed rind model (RPD = 3.97) also demonstrates good predictive ability, though with comparatively higher spectral and compositional variability attributed to disorder-induced optical inconsistencies.

These findings affirm that Vis–NIR spectroscopy, when coupled with effective spectral pretreatments such as SNV, MSC, and Savitzky–Golay smoothing, can provide highly accurate, non-destructive estimation of hue angle (h°) in jackfruit rind. The high Rc^2, Rp^2, and RPD values collectively validate the PLSR model's stability and potential as a predictive tool for assessing rind colour evolution and physiological disorder effects during the 14th week after anthesis.

Table 11: Summary of principal results obtained in the PLS models effects of fruit condition and maturity stages (weeks after anthesis) on rind colour h° of jackfruit cv. Tekam Yellow.

H	WAA	Mean	SD	Rc^2	RMSEc	Rp^2	RMSEp	Bias	Slope	Offset	Cor	RPD
N	10	98.11ab	5.15	0.90	0.96	0.95	0.88	-0.01	0.92	1.83	0.98	11.80
B	10	96.62b	10.36	0.95	0.94	0.86	1.33	-0.20	0.92	1.00	0.93	3.86
N	14	96.73ab	5.44	0.96	0.69	0.90	1.36	0.02	0.94	1.12	0.95	14.78
B	14	88.92c	20.09	0.94	1.09	0.90	1.37	-0.02	0.92	0.96	0.95	3.97

H = Fruit condition, N = Normal, B = Bronzing, WAA = week after anthesis, SD = standard deviation, Cor = correlation, RPD = residual prediction deviation.

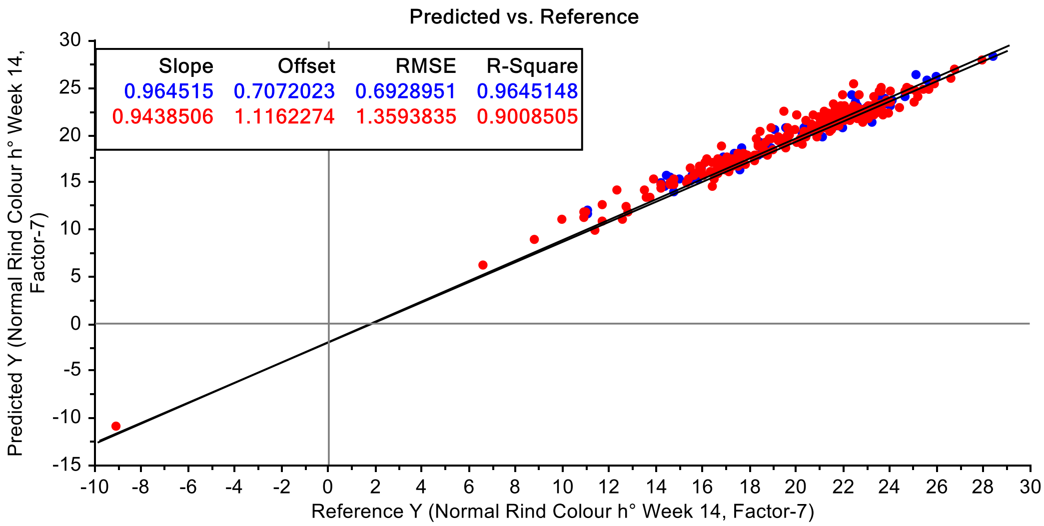

Figure 25: Scatter plots of referenced versus predicted normal rind colour h° in Week 14 using reflectance spectral data with calibration model and prediction model. *• = Calibration Model, • = Prediction Model

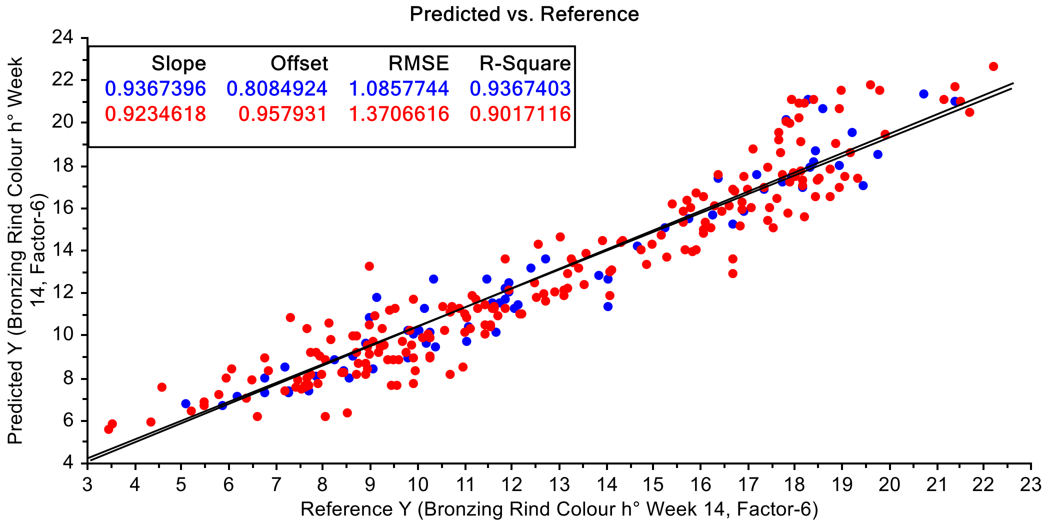

Figure 26: Scatter plots of referenced versus predicted bronzing rind colour h° in Week 14 using reflectance spectral data with calibration model and prediction model. *• = Calibration Model, • = Prediction Model

3.2.12 Predictive performance of PLSR models flesh colour h° at 14 WAA

The results from the calibration and prediction models using Partial Least Squares (PLS) regression within the visible spectral range of 500 to 950 nm indicate that the most effective pretreatment method for predicting the hue angle (h°) of normal jackfruit flesh at Week 14 was the combination of Savitzky–Golay smoothing and Standard Normal Variate (SNV), utilizing seven latent variables (LVs). As shown in Table 12 and Figure 27, the calibration model achieved a coefficient of determination (Rc^2) of 0.95 and a root mean square error of calibration (RMSEc) of 0.92, with the corresponding model equation $y = 0.9456x + 0.4285$. The prediction model also exhibited high performance, with an Rp^2 of 0.94 and an RMSEp of 0.96, and the equation $y = 1.0155x + 0.0044$.

Similarly, for the bronzed jackfruit flesh at Week 14, the same pretreatment approach—Savitzky–Golay and SNV with seven LVs—was found to be optimal. As presented in Table 12 and Figure 28, the calibration model yielded an Rc^2 of 0.94 and an RMSEc of 0.65, with the model equation $y = 0.9404x + 0.4726$. The prediction model achieved an Rp^2 of 0.93 and an RMSEp of 0.73, with the equation $y = 0.9213x + 0.5981$.

The RPD (Residual Prediction Deviation) values further support the robustness of these models, with RPD = 3.90 for normal flesh and RPD = 4.83 for bronzed flesh. Generally, RPD values between 2.5 and 3.0 indicate models suitable for rough screening, while values above 3.0 signify good quantitative predictive capability. Therefore, both models demonstrated excellent predictive accuracy, with the bronzed flesh model performing slightly better in terms of precision and stability. These findings highlight the potential of Vis–NIR spectroscopy, when paired with appropriate pretreatment techniques and PLS regression, as a reliable and accurate method for predicting the hue angle (h°) of jackfruit flesh colour at Week 14.

Table 12: Summary of principal results obtained in the PLS models effects of fruit condition and maturity stages (weeks after anthesis) on flesh colour h° of jackfruit cv. Tekam Yellow.

H	WAA	Mean	SD	Rc^2	RMSEc	Rp^2	RMSEp	Bias	Slope	Offset	Cor	RPD
N	14	83.69b	3.74	0.95	0.92	0.94	0.96	0.12	1.02	0.00	0.97	3.90
B	14	86.02a	3.54	0.94	0.65	0.93	0.73	-0.04	0.92	0.60	0.96	4.83

H = Fruit condition, N = Normal, B = Bronzing, WAA = week after anthesis, SD = standard deviation, Cor = correlation, RPD = residual prediction deviation.

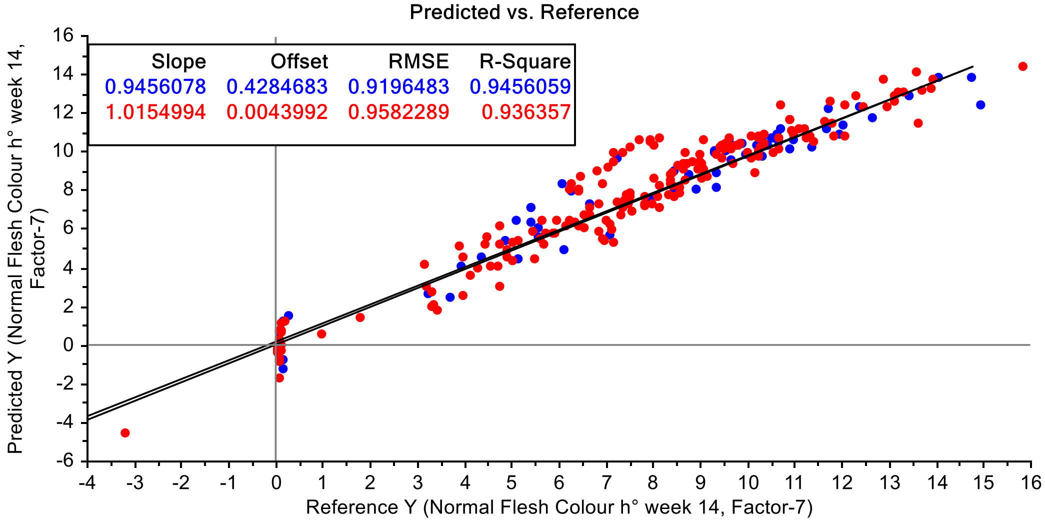

Figure 27: Scatter plots of referenced versus predicted normal flesh colour h° in Week 14 using reflectance spectral data with calibration model and prediction model. *• = Calibration Model, • = Prediction Model

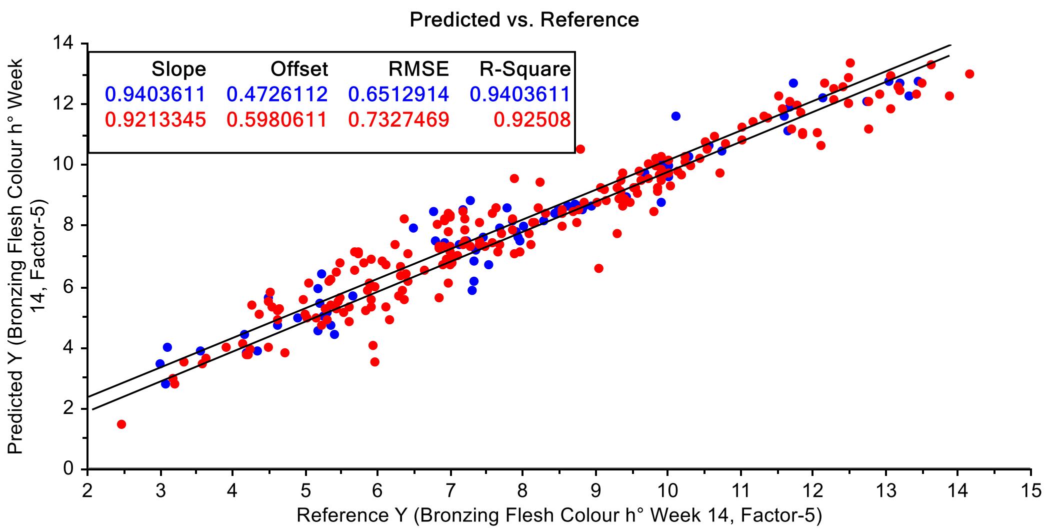

Figure 28: Scatter plots of referenced versus predicted bronzing flesh colour h° in Week 14 using reflectance spectral data with calibration model and prediction model. *• = Calibration Model, • = Prediction Model

3.3 Interpretation and Implication of PLS predictive performance for jackfruit colour attributes

The Partial Least Squares Regression (PLSR) models established using visible–near infrared (Vis–NIR) spectral data demonstrated strong predictive capabilities for colour attributes (L*, a*, b*, C*, and h°) of jackfruit rind and flesh across different maturity stages and fruit conditions (normal and bronzing). The consistent performance trends observed in Tables 1 to 12 and Figures 5 to 28 confirm that the reflectance spectra within 500–950 nm effectively captured chromatic variations associated with pigment accumulation, degradation, and structural tissue differences throughout fruit maturation and bronzing development.

3.3.1 Predictive Performance Across Colour Parameters

Across all colour indices, the PLSR calibration and prediction models exhibited strong linearity and precision, with coefficients of determination (Rc^2 and Rp^2) typically ranging from 0.90 to 0.97 and relatively low root mean square errors (RMSEc and RMSEp) below 1.5. Correspondingly, residual predictive deviation (RPD) values exceeded 3.0 for most parameters, indicating high model robustness according to the classification proposed by [66], where RPD > 3.0 denotes good quantitative prediction and RPD > 5.0 signifies excellent predictive power.

For rind colour, the prediction models for L* and b* showed higher accuracy, particularly for normal fruit samples. These attributes correspond to lightness and yellowness, respectively—key indicators of surface pigmentation resulting from carotenoid accumulation during maturation. The elevated Rc^2 values for L* (0.90–0.96) and b* (0.92–0.95) suggest that Vis–NIR reflectance is sensitive to brightness and yellow hue transitions linked to maturity progression. Conversely, the prediction of a* and h° was slightly less precise in bronzed rind, likely due to irregular oxidative browning and phenolic polymerisation associated with bronzing, which increase spectral scattering and nonlinearity [51].

For flesh colour, PLSR models exhibited even stronger predictive performance, with Rc^2 and Rp^2 often exceeding 0.94 and RPD values ranging between 3.9 and 4.8 (Table 12; Figures 27–28). Among the colour parameters, hue angle (h°) and chroma (C*) were particularly well predicted when using the Savitzky–Golay smoothing combined with Standard Normal Variate (SNV) preprocessing and seven latent variables. This combination effectively minimised baseline drift and scattering caused by variable light penetration through the translucent flesh matrix. Similar outcomes were reported by [12], [15] and [18], who demonstrated that derivative smoothing and SNV correction enhance model robustness for colour estimation in mango and durian flesh. The high RPD (>4.0) values for h° prediction at 14 WAA demonstrate that the Vis–NIR spectra captured fine pigment transitions linked to the yellow–orange hue shift during ripening—a key sensory and commercial quality trait in jackfruit.

3.3.2 Comparative Analysis Between Normal and Bronzing Fruits

Comparative assessment between fruit conditions revealed that normal samples consistently yielded higher Rc^2, Rp^2, and RPD values than bronzed samples for both rind and flesh. This performance gap is attributed to the internal degradation and pigment oxidation occurring in bronzing, which alter the optical scattering pathways and weaken the correlation between spectral response and true colour attributes [8] (Aman *et al.*, 2025). Nevertheless, the bronzed flesh models remained reliable (RPD = 3.5–4.8), confirming that Vis–NIR spectroscopy is sensitive enough to detect subtle chromatic degradation even under physiological stress conditions.

Spectral examination also revealed that bronzed rind exhibited greater noise within the 500–600 nm range—corresponding to chlorophyll and flavonoid absorption regions. This spectral distortion may be linked to the breakdown of photosynthetic pigments and the accumulation of brown phenolic derivatives, similar to phenomena observed in banana peel browning [36] and mango anthracnose infection [54]. These biochemical and structural disturbances contribute to reduced predictive accuracy for a* and h° in bronzed rind, as compared to the more homogeneous flesh tissue.

3.3.3 Implications for Quality Monitoring and Postharvest Handling

The strong prediction performance for L*, b*, and h° parameters highlights the potential of Vis–NIR spectroscopy as a non-destructive grading tool for jackfruit colour evaluation and maturity classification. Since these attributes are closely related to pigment biosynthesis and visual appeal, their accurate prediction allows rapid identification of optimal harvest maturity and early detection of bronzing onset prior to visual manifestation. The application of relatively simple preprocessing (Savitzky–Golay + SNV) ensures the models remain stable across fruit batches, reducing calibration drift and enabling real-time deployment in industrial sorting lines.

These results are consistent with findings in other tropical fruits such as durian [16] and pineapple [26], where Vis–NIR models achieved comparable reliability for colour and quality prediction. The consistency between calibration and prediction equations across rind and flesh tissues further suggests the feasibility of developing integrated calibration models, applicable to mixed tissue reflectance in whole-fruit evaluation systems. This approach could streamline industrial inspection processes and improve overall postharvest management efficiency.

3.3.4 Broader Scientific and Practical Significance

The present study reinforces that visible-range spectral information (500–950 nm) alone is adequate for modelling pigment-based quality traits in large, heterogeneous tropical fruits such as jackfruit. This observation supports earlier work by [48] and [56], who demonstrated that visible bands are sufficient for pigment and structural assessments when near-infrared moisture interference is limited. The high prediction performance for hue and chroma indicates that spectral features in this region effectively represent the biochemical basis of colour—primarily carotenoid, chlorophyll, and phenolic transitions—without the need for extended NIR wavelengths.

From a scientific standpoint, these findings validate the relationship between spectral reflectance and tissue microstructure, where pigment concentration and chromatic stability govern the spectral response. The capacity to model both normal and bronzed tissues using consistent latent variables also highlights the adaptability of PLSR modelling in handling biological variability. The successful prediction of h° and C* across tissues demonstrates that Vis–NIR spectroscopy not only quantifies external appearance but also provides insight into internal pigment dynamics relevant to physiological disorders and ripening behaviour.

4. Discussion

The absorption feature near 680 nm in the rind spectra likely corresponds to chlorophyll, which contributes to the green hue in immature jackfruit, consistent with [17]. A pronounced band at ~940 nm, observed in both rind and flesh, indicates water absorption, corroborating earlier findings in apple fruit [45]. The 550 nm peak in the flesh spectra is attributed to carotenoids, while the gradual slope toward 940 nm may reflect anthocyanin absorption [35, 53 & 65], confirming the role of pigment composition in spectral variability.

PLSR models developed from rind and flesh spectra across 10–14 WAA maturity stages accurately predicted internal attributes. Among twelve preprocessing combinations, Savitzky–Golay with SNV and 2nd Derivative with MSC achieved superior calibration performance by minimizing baseline drift and light scattering. Optimal models used seven latent variables, balancing accuracy and complexity.

Rind colour parameters (L*, a*, b*, C*, h°, ΔE) varied significantly with maturity and bronzing. Immature fruit (10 WAA) showed high L* and low a* values, transitioning to yellowish hues by 14 WAA. Bronzed samples exhibited lower L* and higher a*, reflecting oxidation-induced pigment degradation. These spectral–chromatic relationships align with citrus and apple studies linking colour shifts to internal disorder [11 &13].

For flesh, SG+SNV and 2nd Derivative+MSC preprocessing yielded the most accurate models, particularly at 12–14 WAA. Healthy tissues displayed bright yellow pigmentation (high L*, b*, C*), whereas bronzed flesh showed reduced brightness and higher ΔE, consistent with carotenoid loss and enzymatic browning

[41 & 61]. The second derivative enhanced pigment-related absorption resolution, while MSC corrected scattering from structural degradation.

Overall, Vis–NIR spectroscopy effectively captured maturity- and disease-related chromatic transitions. Mean L* declined from 77.4 (10 WAA healthy) to 64.4 (14 WAA bronzed), while h° shifted from 95° to 70°, indicating pigment breakdown and browning onset. ΔE values exceeding 6.0 confirmed perceptible visual deviations, enabling reliable non-destructive discrimination of bronzed fruit. Reduced L* and h° reflect oxidative degradation of chlorophylls and carotenoids [14 & 38], consistent with reddish-brown discoloration reported by [69].

PLSR calibration yielded R^2 values of 0.87–0.92 and RPD >2.5, demonstrating robust predictive performance comparable to that reported for apple and mango [52]. These findings confirm the capability of Vis–NIR spectroscopy to non-destructively detect pigment degradation, maturity progression, and bronzing symptoms in *Artocarpus heterophyllus* cv. Tekam Yellow.

5. Conclusions

This study demonstrated the feasibility of visible–near infrared (Vis-NIR) spectroscopy coupled with partial least squares regression (PLSR) for non-destructive prediction of key physicochemical and biochemical attributes in jackfruit (*Artocarpus heterophyllus* Lam. cv. Tekam Yellow). Strong predictive performance was achieved for colour metrics, particularly in flesh tissues, where $R^2>0.85$ and RPD ≥ 2.0 indicated robust model reliability. Effective preprocessing—especially Savitzky–Golay smoothing with SNV or MSC, and second-derivative transformations—significantly improved calibration accuracy by minimizing scatter and enhancing chemical signal fidelity.

Bronzing disorder introduced spectral variability and reduced model stability, particularly for colour metrics, underscoring the need to account for physiological conditions during calibration. Diseased fruits exhibited diminished colour metrics, consistent with tissue degradation and metabolic impairment. Tissue type and maturity stage (10–14 WAA) further influenced prediction accuracy, with the flesh showing superior spectral responsiveness compared with rind and seed due to higher water content and optical homogeneity.

Overall, Vis-NIR spectroscopy proved a reliable and scalable approach for rapid, non-invasive assessment of internal and external jackfruit quality, supporting sustainable postharvest grading and processing. Future research should expand calibration datasets to include seasonal and regional variability, integrate hybrid models (e.g., SVM, ANN), and employ adaptive or condition-stratified calibration to enhance prediction robustness under field conditions.

To improve pH and titratable acidity prediction, stratified PLS modeling by fruit condition (healthy vs. bronzed) and maturity stage is recommended, or alternatively, inclusion of categorical covariates for disease status. Calibration sets should encompass broad chemical and pathological variability, while preprocessing optimization and variable selection (VIP, selectivity ratio) should target late-maturity and bronzed samples. Routine model updating is essential to maintain performance across seasons and orchards.

The present work is limited by cultivar and maturity range (10–14 WAA), restricting model extrapolation. Some bronzing-affected subsets yielded Rp^2 and RPD values below robust thresholds, warranting cautious application. Broader sampling and continuous maturity tracking are needed to refine spectral–biochemical relationships and enable hierarchical or functional PLS modeling for real-time implementation in jackfruit quality monitoring systems.

In conclusion, the PLSR models developed in this study exhibited excellent predictive capability for the colour parameters of both rind and flesh, regardless of fruit condition. The superior model performance for flesh colour, particularly for h° and C*, underscores the method's sensitivity to pigment transformation associated with maturity progression and bronzing incidence. These results affirm that Vis–NIR spectroscopy, combined with appropriate preprocessing techniques, provides a rapid, reliable, and non-destructive alternative for monitoring jackfruit colour quality—supporting its application in maturity classification, quality control, and early disorder detection.

Author Contributions Declaration

Conceptualization, **Kok Jeng Lim**, **Phebe Ding**, and **Nazmi Mat Nawi**; Literature review and data collection, **Kok Jeng Lim**; Writing – original draft, **Kok Jeng Lim**; Writing – review and editing, **Phebe Ding**, **Nazmi Mat Nawi**, and **Mashitah Jusoh**; Supervision, **Phebe Ding**, **Nazmi Mat Nawi**, and **Mashitah Jusoh**. Funding acquisition: not applicable.

Data Availability Declaration

The datasets generated during and/or analyzed during the current study are available.

Funding Declaration

This research did not receive any specific grant from funding agencies in the public, commercial, or not-for-profit sectors.

Declaration of Competing Interest

The authors declare that there are no known financial conflicts of interest or personal relationships that could have influenced the research, analysis, or interpretation of data presented in this manuscript.

Declaration of Ethical Approval

Not applicable.

Declaration of Consent to Participate

Not applicable.

Declaration of Consent for Publication

Not applicable.

Acknowledgements

The authors sincerely express their gratitude to the Department of Crop Science, Faculty of Agriculture; the Department of Biological and Agricultural Engineering, Faculty of Engineering; and the Institute of Plantation Studies at Universiti Putra Malaysia for their invaluable technical assistance and logistical support throughout the course of this research.

References

[1] Abdullah, N., Nawi, N. M., Ding, P., Kassim, M. S. M., & Lazim, S. S. R. M. (2021). Prediction of soluble solids content of jackfruit from skin surface using spectroscopic method. *Agricultural Mechanization in Asia, Africa and Latin America*, *52*(3), 4013-21.

[2] Abdullah, N. (2019). Application of shortwave near infrared spectroscopy in determining physicochemical properties of jackfruit [Master]. Universiti Putra Malaysia.

[3] Abidin, N., Ismail, S. I., Vadamalai, G., Yusof, M. T., Hakiman, M., Karam, D. S., Ismail-Suhaimy, N. W., Ibrahim, R., & Zulperi, D. (2020). Genetic diversity of *Pantoea stewartii* subspecies *stewartii* causing jackfruit-bronzing disease in Malaysia. *PLOS ONE*, *15*(6), e0234350. Available: https://doi.org/10.1371/journal.pone.0234350

[4] Afonso, A. M., Antunes, M. D., Cruz, S., Cavaco, A. M., & Guerra, R. (2022). Non-destructive follow-up of 'Jintao' kiwifruit ripening through VIS-NIR spectroscopy–individual vs. average calibration model's

predictions. *Postharvest Biology and Technology*, *188*, 111895. Available: https://doi.org/10.1016/j.postharvbio.2022.111895
[5] Al-Harrasi, A., Rehman, N.U., Mabood, F., Albroumi, M., Ali, L., Hussain, J., & Alameri, S. (2017). Application of NIRS coupled with PLS regression as a rapid, non-destructive alternative method for quantification of KBA in Boswellia Sacra. Spectrochimica Acta Part A: *Molecular and Biomolecular Spectroscopy*, 184, 277-285. Available: https://doi.org/10.1016/j.saa.2017.05.018

[6] Al Riza, D. F., Rulin, C., Tun, N. T. T., Yi, P. P. L., Thwe, A. A., Myint, K. T., & Kondo, N. (2023). Mango (Mangifera indica cv. Sein Ta Lone) ripeness level prediction using color and textural features of combined reflectance-fluorescence images. *Journal of Agriculture and Food Research*, *11*, 100477. Available: https://doi.org/10.1016/j.jafr.2022.100477

[7] Ali, M. M., Hashim, N., & Shahamshah, M. I. (2021). Durian (*Durio zibethinus*) ripeness detection using thermal imaging with multivariate analysis. *Postharvest Biology and Technology*, *176*, 111517. Available: https://doi.org/10.1016/j.postharvbio.2021.111517

[8] Aman, M., Khan, Z. U., Khan, J., Mashori, A. S., Ali, A., Jabeen, N., ... & Li, F. (2025). A Comprehensive Review on Crop Stress Detection: Destructive, Non-Destructive, and ML-Based Approaches. *Frontiers in Plant Science*, *16*, 1638675.Available: https://doi.org/10.3389/fpls.2025.1638675

[9] Babu, P. S., Sudheer, K. P., Sarathjith, M. C., Mathew, S. M., & Gopinath, G. (2020). Quality evaluation of tender jackfruit using near-infrared reflectance spectroscopy. *Journal of Applied Horticulture*, 22(3), 171-175. Available: https://doi.org/10.37855/jah.2020.v22i03.31

[10] Boardman, A. E., Hui, B. S. and Wold, H. (1981). The partial least squares-fix point method of estimating interdependent systems with latent variables. *Communications in statistics-theory and methods*, *10*(7), 613-639. Available: https://doi.org/10.1080/03610928108828062

[11] Cayuela, J. A. (2008). Vis/NIR soluble solids prediction in intact oranges (Citrus sinensis L.) cv. Valencia Late by reflectance. *Postharvest Biology and Technology*, *47*(1), 75-80. Available: https://doi.org/10.1016/j.postharvbio.2007.06.005

[12] Cheng, J. H., & Sun, D. W. (2017). Partial least squares regression (PLSR) applied to NIR and HSI spectral data modeling to predict chemical properties of fish muscle. *Food engineering reviews*, *9*(1), 36-49. Available: https://doi.org/10.1007/s12393-016-9147-1

[13] Clark, C. J., McGlone, V. A., & Jordan, R. B. (2003). Detection of brown heart in 'Braeburn' apple by transmission NIR spectroscopy. *Postharvest Biology and Technology*, *28*(1), 87-96. Available: https://doi.org/10.1016/S0925-5214(02)00122-9

[14] Dias, C., Brandão, T. R., Cassoni, C., Vasconcelos, M. W., Ferrante, A., & Pintado, M. (2023). Firmness prediction of 'Rocha' pear based on non-destructive methods and shelf-life using PLS-regression modeling. *Postharvest Biology and Technology*, *205*, 112493. Available: https://doi.org/10.1016/j.postharvbio.2023.112493

[15] Diop, A., Méot, J. M., Lechaudel, M., Chiroleu, F., Ndiaye, N. D., Mertz, C., ... & Chillet, M. (2021). Impact of preharvest and postharvest on color changes during convective drying of mangoes. *Foods*, *10*(3), 490. Available: https://doi.org/10.3390/foods10030490

[16] Ditcharoen, S., Sirisomboon, P., Saengprachatanarug, K., Phuphaphud, A., Rittiron, R., Terdwongworakul, A., ... & Posom, J. (2023). Improving the non-destructive maturity classification model for durian fruit using near-infrared spectroscopy. *Artificial Intelligence in Agriculture*, *7*, 35-43. Available: https://doi.org/10.1016/j.aiia.2023.02.002

[17] ElMasry, G., Wang, N., ElSayed, A., & Ngadi, M. (2007). Hyperspectral imaging for nondestructive determination of some quality attributes for strawberry. *Journal of Food Engineering*, 81(1), 98-107. Available: https://doi.org/10.1016/j.jfoodeng.2006.10.016

[18] Elsayed, S., Gala, H., Abd El-baki, M. S., Maher, M., Elbeltagi, A., Salem, A., ... & Abd El-Fattah, N. G. (2025). Hyperspectral technology and machine learning models to estimate the fruit quality parameters of mango and strawberry crops. *PloS one*, *20*(2), e0313397. Available: https://doi.org/10.1371/journal.pone.0313397

[19] Elsherbiny, O., El-Hendawy, S., Elsayed, S., Elwakeel, A. E., Alebidi, A., Yue, X., ... & Galal, H. (2025). Incorporation of visible/near-infrared spectroscopy and machine learning models for indirect assessment of grape ripening indicators. *Scientific Reports*, *15*(1), 12345. Available: https://doi.org/10.1038/s41598-024-81694-3

[20] Fan, S., Wang, Q., Tian, X., Yang, G., Xia, Y., Li, J., & Huang, W. (2020). Non-destructive evaluation of soluble solids content of apples using a developed portable Vis/NIR device. Biosystems Engineering, 193, 138-148. Available: https://doi.org/10.1016/j.biosystemseng.2020.02.017

[21] Gapasin, R. M., Garcia, R. P., Advincula, C. T., De la Cruz, C. S. & Borines, L. M. (2014). Fruit bronzing: A new disease affecting jackfruit caused by *Pantoea stewartii* (Smith) Mergaert *et al.*, *Annals of Tropical Research*, 36: 17-31, Available: https://doi.org/10.32945/atr3612.2014

[22] Giovanelli, G., Sinelli, N., Beghi, R., Guidetti, R., & Casiraghi, E. (2014). NIR spectroscopy for the optimization of postharvest apple management. *Postharvest Biology and Technology*, *87*, 13-20. Available: https://doi.org/10.1016/j.postharvbio.2013.07.041

[23] Golic, M., & Walsh, K. B. (2006). Robustness of calibration models based on near infrared spectroscopy for the in-line grading of stonefruit for total soluble solids content. *Analytica chimica acta*, *555*(2), 286-291. Available: https://doi.org/10.1016/j.aca.2005.09.014

[24] Gómez, A. H., He, Y., & Pereira, A. G. (2006). Non-destructive measurement of acidity, soluble solids and firmness of Satsuma mandarin using Vis/NIR-spectroscopy techniques. *Journal of food engineering*, *77*(2), 313-319. Available: https://doi.org/10.1016/j.jfoodeng.2005.06.036 pg 2

[25] Grabska, J., Beć, K. B., Ueno, N., & Huck, C. W. (2023). Analyzing the quality parameters of apples by spectroscopy from Vis/NIR to NIR region: A comprehensive review. *Foods*, *12*(10), 1946. Available: https://doi.org/10.3390/foods12101946

[26] Gupta, A. K., Koch, P., Yumnam, M., Medhi, M., Madufor, N. J., Opara, U. L., & Mishra, P. (2022). Biosensors involved in fruit and vegetable processing industries. In *Biosensors in Food Safety and Quality* (pp. 111-134). CRC Press.

[27] Guthrie, J. A., Reid, D. J., & Walsh, K. B. (2005). Assessment of internal quality attributes of mandarin fruit. 2. NIR calibration model robustness. *Australian Journal of Agricultural Research*, *56*(4), 417-426. Available: https://doi.org/10.1071/AR04299

[28] Hernandez-Morales A., Perez-Casillas J. M., Soria-Guerra R. E., Velazquez-Fernandez J. B., & Arvizu-Gomez J. L. (2017). First report of *Pantoea stewartii* subspecies *stewartii* causing jackfruit bronzing disease in Mexico. *Journal of Plant Pathology*, 99, 799–818. Available: https://doi.org/10.4454/JPP.V9913.3969

[29] Huang, Y., Zheng, Y., Liu, P., Xie, L., & Ying, Y. (2025). Enhanced prediction of soluble solids content and vitamin C content in citrus using visible and near-infrared spectroscopy combined with one-dimensional convolutional neural network. *Journal of Food Composition and Analysis*, *139*, 107131. Available: https://doi.org/10.1016/j.jfca.2024.107131

[30] Ibrahim, R., Ismail-Suhaimy, N. W., Shu-Qing, T., Ismail, S. I., Abidin, N., Hakiman, M., Karam, D. S., Ahmad-Hamdani, M. S., Yusof, M. T., & Zulperi, D. (2020). Molecular characterization and phylogenetic analysis of

Pantoea stewartii subspecies *stewartii* causing bronzing disease of jackfruit in Malaysia based on *cps* and *hrp* gene sequences. *Journal of Plant Pathology*, *102*(1), 193–199. Available: https://doi.org/10.1007/s42161-019-00383-7

[31] Kaur, J., Singh, Z., Shah, H. M. S., Mazhar, M. S., Hasan, M. U., & Woodward, A. (2024). Insights into phytonutrient profile and postharvest quality management of jackfruit: A review. *Critical Reviews in Food Science and Nutrition*, *64*(19), 6756-6782. Available: https://doi.org/10.1080/10408398.2023.2174947

[32] Kiran, P. R., Yeasin, M., Aradwad, P., Arunkumar, T. V. & Parray, R. A. (2024). Advancing mango quality assurance: Non-destructive detection of spongy tissue using visible near-infrared spectroscopy and machine learning classification. *Future Postharvest and Food*, *1*(2), 237-251. Available: https://doi.org/10.1002/fpf2.12023

[33] Kim, G. Y., Lee, K. J., Choi, K. H., Son, J. R., Choi, D. S. & Kang, S. W. (2004). Defect and ripeness inspection of citrus using NIR transmission spectrum. *Key engineering materials*, *270*, 1008-1013. Available: https://doi.org/10.4028/www.scientific.net/KEM.270-273.1008

[34] Lovász, T., Merész, P., & Salgó, A. (1994). Application of near infrared transmission spectroscopy for the determination of some quality parameters of apples. *Journal of Near Infrared Spectroscopy*, *2*(4), 213-221. Available: https://doi.org/10.1255/jnirs.47

[35] Lu, W., Shi, Y., Wang, R., Su, D., Tang, M., Liu, Y., & Li, Z. (2021). Antioxidant activity and healthy benefits of natural pigments in fruits: A review. *International journal of molecular sciences*, *22*(9), 4945. Available: https://doi.org/10.3390/ijms22094945

[36] Ma, H., Hu, L., Zhao, J., He, J., Wen, A., Lv, D., ... & Pan, L. (2025). Comparative Analysis of Chilling Injury in Banana Fruit During Storage: Physicochemical and Microstructural Changes, and Early Optical-Based Nondestructive Identification. *Foods*, *14*(8), 1319. Available: https://doi.org/10.3390/foods14081319

[37] Magwaza, L. S., Opara, U. L., Terry, L. A., Landahi, S., Cronje, P. J. R., Nieuwoudt, H. H., Hanssens, A., Saeys, W., & Nicolaï, B. M. (2013). Evaluation of Fourier transform-NIR spectroscopy for integrated external and internal quality assessment of 'Valencia' oranges. *Journal of Food Composition Analysis*, 31, 144-154. Available: https://doi.org/10.1016/j.jfca.2013.05.007

[38] Magwaza, L. S., Opara, U. L., Cronje, P. J., Landahl, S., Nieuwoudt, H. H., Mouazen, A. M., & Terry, L. A. (2014). Assessment of rind quality of 'Nules Clementine' mandarin fruit during postharvest storage: 2. Robust Vis/NIRS PLS models for prediction of physico-chemical attributes. *Scientia Horticulturae*, *165*, 421-432. Available: https://doi.org/10.1016/j.scienta.2013.09.050

[39] Maniwara, P., Nakano, K., Boonyakiat, D., Ohasi, S., Hiroi, M., & Tohyama, T. (2014). The use of visible and near infrared spectroscopy for evaluating passion fruit postharvest quality. *Journal of Food Engineering*, 143, 33-43. Available: https://doi.org/10.1016/jfoodeng.2014.06.028

[40] McGlone, V. A., Jordan, R. B., Seelye, R., & Martinsen, P. J. (2002). Comparing density and NIR methods for measurement of kiwifruit dry matter and soluble solids content. *Postharvest Biology and Technology*, *26*(2), 191-198. Available: https://doi.org/10.1016/S0925-5214(02)00014-5

[41] McGlone, V. A., Fraser, D. G., Jordan, R. B., & Künnemeyer, R. (2003). Internal quality assessment of mandarin fruit by vis/NIR spectroscopy. *Journal of Near Infrared Spectroscopy*, *11*(5), 323-332. Available: https://doi.org/10.1255/jnirs.383

[42] McGlone, V. A., Martinsen, P. J., Clark, C. J., & Jordan, R. B. (2005). On-line detection of Brownheart in Braeburn apples using near infrared transmission measurements. *Postharvest biology and technology*, *37*(2), 142-151. Available: https://doi.org/10.1016/j.postharvbio.2005.04.011

[43] Mishra, P., Woltering, E., Brouwer, B., & Hogeveen-van Echtelt, E. (2021). Improving moisture and soluble solids content prediction in pear fruit using near-infrared spectroscopy with variable selection and model updating

approach. *Postharvest Biology and Technology*, *171*, 111348. Available: https://doi.org/10.1016/j.postharvbio.2020.111348

[44] Naes, T., Isaksson, T., Fearn, T., & Davies, T. (2004). A user-friendly guide to multivariate calibration and classification. Chichester, United Kingdom: *Near Infrared Spectroscopy Publications*, 420.

[45] Nagy, A., Riczu, P., & Tamas, J. (2016). Spectral evaluation of apple fruit ripening and pigment content alteration. *Scientia Horticulturae*, *201*, 256-264. Available: https://doi.org/10.1016/j.scienta.2016.02.016

[46] Nicolaï, B. M., Beullens, K., Bobelyn, E., Peirs, A., Saeys, W., & Theron, K. I. (2007). Non-destructive measurement of fruit and vegetable quality by means of NIR spectroscopy: A Review. *Postharvest Biology and Technology*, 46(2), 99-118. Available: https://doi.org/10.1016/j.postharvbio.2007.06.024

[47] Nicolaï, B. M., Verlinden, B. E., Desmet, M., Saevels, S., Saeys, W., Theron, K., & Torricelli, A. (2008). Time-resolved and continuous wave NIR reflectance spectroscopy to predict soluble solids content and firmness of pear. *Postharvest Biology and Technology*, *47*(1), 68-74. Available: https://doi.org/10.1016/j.postharvbio.2007.06.001

[48] Nicolaï, B. M., Defraeye, T., De Ketelaere, B., Herremans, E., Hertog, M. L., Saeys, W., ... & Verboven, P. (2014). Nondestructive measurement of fruit and vegetable quality. *Annual review of food science and technology*, *5*(1), 285-312. Available: https://doi.org/10.1146/annurev-food-030713-092410

[49] Onsawai, P., Phetpan, K., Khurnpoon, L., & Sirisomboon, P. (2021). Evaluation of physiological properties and texture traits of durian pulp using near-infrared spectra of the pulp and intact fruit. *Journal of Measurement*, 174, 1-9. Available: https://doi.org/10.1016/j.measurement.2020.108684

[50] Osborne, B. G., Fearn, T., & Hindle, P. H. (1993). *Practical NIR spectroscopy with applications in food and beverage analysis* (pp. 227-pp). ISBN (Hardback): 978-0-582-09946-3.

[51] Pandiselvam, R., Prithviraj, V., Manikantan, M. R., Kothakota, A., Rusu, A. V., Trif, M., & Mousavi Khaneghah, A. (2022). Recent advancements in NIR spectroscopy for assessing the quality and safety of horticultural products: A comprehensive review. *Frontiers in Nutrition*, *9*, 973457.Available: https://doi.org/10.3389/fnut.2022.973457

[52] Peirs, A., Tirry, J., Verlinden, B., Darius, P., & Nicolaï, B. M. (2003). Effect of biological variability on the robustness of NIR models for soluble solids content of apples. *Postharvest Biology and Technology*, 28(2), 269-280. Available: https://doi.org/10.1016/S0925-5214(02)00196-5

[53] Pervaiz, T., Songtao, J., Faghihi, F., Haider, M. S., & Fang, J. (2017). Naturally occurring anthocyanin, structure, functions and biosynthetic pathway in fruit plants. *J. Plant Biochem. Physiol*, *5*(2), 1-9. Available: https://doi.org/10.4172/2329-9029.1000187

[54] Rayhana, R., Ma, Z., Liu, Z., Xiao, G., Ruan, Y., & Sangha, J. S. (2023). A review on plant disease detection using hyperspectral imaging. *IEEE Transactions on AgriFood Electronics*, *1*(2), 108-134. Available: https://doi.org/10.1109/TAFE.2023.3329849

[55] Rinnan, Å., Berg, F. V. D., & Engelsen, S. B. (2009). Review of the most common pre- processing techniques for near-infrared spectra. TrAC, Trends in Analytical Chemistry, 28(10), 1201–1222. Available: https://doi.org/10.1016/j.trac.2009.07.007

[56] Saad, A., Azam, M. M., & Amer, B. M. (2022). Quality analysis prediction and discriminating strawberry maturity with a hand-held Vis–NIR spectrometer. *Food Analytical Methods*, *15*(3), 689-699. Available: https://doi.org/10.1007/s12161-021-02166-2

[57] Saechua, W., Sharma, S., Nakawajana, N., Leepaitoon, K., Chunsri, R., Posom, J., & Pornchaloempong, P. (2021). Integrating Vis-SWNIR spectrometer in a conveyor system for in-line measurement of dry matter content and soluble solids content of durian pulp. *Postharvest Biology and Technology*, *181*, 111640. Available: https://doi.org/10.1016/j.postharvbio.2021.111640

[58] Saeys, W., Mouazen, A. M., & Ramon, H. (2005). Potential for onsite and online analysis of pig manure using visible and near infrared reflectance spectroscopy. *Biosystems Engineering*, 91(4), 393-402. Available: https://doi.org/10.1016/j.biosystemseng.2005.05.001

[59] Saeys, W., Velazco-Roa, M. A., Thennadil, S. N., Ramon, H., & Nicolaï, B. M. (2008). Optical properties of apple skin and flesh in the wavelength range from 350 to 2200 nm. *Applied optics*, *47*(7), 908-919. Available: https://doi.org/10.1364/AO.47.000908

[60] Saranwong, I., Sornsrivichai, J., & Kawano, S. (2003). Performance of a portable near infrared instrument for Brix value determination of intact mango fruit. *Journal of near infrared spectroscopy*, *11*(3), 175-181. Available: https://doi.org/10.1255/jnirs.364

[61] Saranwong, S., Sornsrivichai, J., & Kawano, S. (2004). Prediction of ripe-stage eating quality of mango fruit from its harvest quality measured nondestructively by near infrared spectroscopy. *Postharvest biology and technology*, *31*(2), 137-145. Available: https://doi.org/10.1016/j.postharvbio.2003.08.007

[62] Sarkar, S., Basak, J. K., Moon, B. E., & Kim, H. T. (2020). A comparative study of PLSR and SVM-R with various preprocessing techniques for the quantitative determination of soluble solids content of hardy kiwi fruit by a portable Vis/NIR spectrometer. *Foods*, *9*(8), 1078. Available: https://doi.org/10.3390/foods9081078

[63] Silva, M. F. D., Roque, J. V., Soares, J. M., Moura, L. D. O., Medeiros, A. D. D., Silva, F. L. D., & Silva, L. J. D. (2023). Near infrared spectroscopy for the classification of vigor level of soybean seed. *Revista Ciência Agronômica*, *55*, e20238703. Available: https://doi.org/10.5935/1806-6690.20240005

[64] Sirisomboon, P., & Nawayon, J. (2017). Evaluation of soluble solids of curry soup containing coconut milk by near infrared spectroscopy. *Journal of Near Infrared Spectroscopy*, *25*(3), 203-210. Available: https://doi.org/10.1177/0967033517711472

[65] Van Beers, R., Aernouts, B., Watté, R., Schenk, A., Nicolaï, B. and Saeys, W. (2017). Effect of maturation on the bulk optical properties of apple skin and cortex in the 500–1850 nm wavelength range. *Journal of Food Engineering*, 214, 79-89. Available: https://doi.org/10.1016/j.jfoodeng.2017.06.013

[66] Williams, P., & Norris, K. (1987). *Near-infrared technology in the agricultural and food industries*.

[67] Yu, S., Huan, K., Liu, X., Wang, L., & Cao, X. (2023). Quantitative model of near infrared spectroscopy based on pretreatment combined with parallel convolution neural network. *Infrared Physics & Technology*, *132*, 104730. Available: https://doi.org/10.1016/j.infrared.2023.104730

[68] Zeaiter, M., Roger, J. M., Bellon-Maurel, V., & Rutledge, D. N. (2004). Robustness of models developed by multivariate calibration. Part I: The assessment of robustness. *TrAC Trends in Analytical Chemistry*, *23*(2), 157-170. Available: https://doi.org/10.1016/S0165-9936(04)00307-3

[69] Zulperi, D., Manaf, N., Ismail, S. I., Karam, D. S., & Yusof, M. T. (2017). First Report of *Pantoea stewartii* subsp. *stewartii* Causing Fruit Bronzing of Jackfruit (*Artocarpus heterophyllus*), a New Emerging Disease in Peninsular Malaysia. *Plant Disease*, *101*(5), 831–831. Available: https://doi.org/10.1094/PDIS-11-16-1689-PDN

Conflict of Interest: The authors declare that the research was conducted in the absence of any commercial or financial relationship that could be construed as a potential conflict of interest.